

IN VITRO CYTOTOXICITY TESTS OF NANOMATERIALS ON 3T3 AND L929
CANCEROUS CELLS

A Thesis by

Madhulika Srikanth

Mechanical Engineering, Wichita State University, 2012

Submitted to the Department of Mechanical Engineering
and the faculty of the Graduate School of
Wichita State University
in partial fulfilment of
the requirements for the degree of
Masters of Science

May 2012

© Copyright 2012 by Madhulika Srikanth

All Rights Reserved

IN VITRO CYTOTOXICITY TESTS OF NANOMATERIALS ON 3T3 AND L929
CANCEROUS CELLS

The following faculty members have examined the final copy of this thesis for form and content, and recommend that it be accepted in partial fulfilment of the requirement for the degree of Master of Science, with a major in Mechanical Engineering.

Ramazan Asmatulu, Committee Chair

S.Y. Yang, Committee Member

T. S. Ravigururajan, Committee Member

DEDICATION

To my parents, friends and well-wishers.

ACKNOWLEDGEMENTS

I would like to thank my advisor and committee chair, Dr. Ramazan Asmatulu, for his unfailing support and guidance throughout this project. I would also like to thank Dr. Yang for making all the facilities in the Biology lab available to carry out the experiment. I am highly in debt to Zheng Song, who guided me step by step and backed me up through the whole process. This wouldn't have been possible without her. I would also like to thank Dr. Heath Misak who helped me initiate the project and supported me through it. I would also like to thank Dr. Ravigururajan for his valuable suggestions. Last but not the least; I would like to thank my friend Vishal Nageshkar for proof reading the report and give new ideas.

ABSTRACT

In this MS thesis, cytotoxicity tests of various nanomaterials, which have commercial applications and involve a contact with human body, were performed at different conditions. The nanomaterials used for the experiments included pristine 100 ply carbon nanowire, graphene nanoflakes, multiwall carbon nanotubes, nanoclay and C₆₀ (buckyball or fullerene). The nanomaterials cytotoxicities were calculated and compared to each other using human and mice fibroblast cancerous cells (3T3 and L929 resp.). The in vitro MTT Assay was used as the testing method because of its simplicity and reliability. The results were analyzed by means of a spectrophotometer at 590 nm wavelength. From the optical density studies, the viabilities were calculated and the toxicities of those nanomaterials were compared.

Pristine 100 ply carbon nanowire was the most viable nanomaterial with the average viability value of 86.9%. The effect of dilution on carbon nanowire was negligible which may have be due to its single dimensional threaded structure. This structure also reduced its toxicity values. However, with increase in time duration this structure became slightly weaker, and the nanowires unwound and dispersed into the media, leading to a slight increase in cytotoxicity. The concentration of the carbon nanowire at which the MTT test was conducted was 3 cm²/ml (external surface area) which weighed 18.52 mg/ml. The second most viable material after the carbon nanowire was fullerene with a viability of 75.2%. Its close packed 3D structure, negative charge and hydrophobicity may have contributed to the low cytotoxic behaviour of this nanomaterial. It was also observed that with the decrease in concentration there was a steep increase in the viability of the cells. By decreasing the concentration from 10.00 mg/ml to 2.00 mg/ml, the viability of fullerene was increased from 75% to 85%. The viabilities of other nanomaterials were in the order of multiwall carbon nanotubes (69.75%), graphene (67.48%) and nanoclay (61.34%). By decreasing the concentration from 1.10 mg/ml to 0.58 mg/ml, the viability was increased from 70% to 80%.

TABLE OF CONTENTS

CHAPTER	PAGE
1. INTRODUCTION	1
1.1 Background	1
1.2 Motivation	2
1.3 Goals	2
2. LITERATURE REVIEW	3
2.1 Carbon Nanowires	3
2.1.1 Applications of Carbon Nanowire	3
2.2 Carbon Nanotubes	4
2.2.1 Applications of Carbon Nanotubes	5
2.3 Graphene	8
2.3.1 Applications of Graphene	8
2.4 Fullerene	9
2.4.1 Applications of Fullerene	10
2.5 Nanoclay	12
2.6 Cytotoxicity	13
2.7 Types of Cytotoxic Assays	15
2.7.1 Trypan Blue	15
2.7.2 Lactate Dehydrogenase (LDH)	16
2.7.3 Sulphorhodamine B Assay	16
2.7.4 Electric Cell Substrate Impedance Sensing (ECIS) Assay	17
2.7.5 Colonogenic Assay	18
2.7.6 Water Soluble Tetrazolium (WST) Assay	19
2.7.7 MTT or MTS Assay	20
2.8 Optical Density	21
2.9 Harmful Effects of Toxic Nanomaterials	22
2.9.1 Respiratory Cytotoxicity	22
2.9.2 Fibroblast and Skin Cytotoxicity	24
2.9.3 Neural Cytotoxicity	25
2.9.4 Cytotoxicity on Human Circulatory System	26
2.9.5 Toxic Effects on DNA	27
2.10 Reasons for Cytotoxicity	28
2.11 Mode of Transport of Nanomaterial within Human Body	28
2.12 Usefulness of Cytotoxicity	30
2.13 Protection and Preventive Measures	30
3. EXPERIMENT	33
3.1 Basis of Experiment	33
3.2 Materials Required	34
3.3 Experimental Procedure	36

TABLE OF CONTENTS (continued)

CHAPTER	PAGE
4. RESULTS AND ANALYSIS	43
4.1 Preliminary Results	43
4.2 Main Results	45
4.2.1 OD590 - Nanowire - 3T3	48
4.2.2 OD590 - Graphene - 3T3	48
4.2.3 OD590 - Nanowire - 3T3	49
4.2.4 Viability Graph - Nanowire - 3T3	49
4.2.5 Viability Graph - Graphene - 3T3	50
4.2.6 Viability Graph - Nanotubes - 3T3	51
4.2.7 OD590 - Nanowire - L929	53
4.2.8 OD590 - Graphene - L929	54
4.2.9 OD590 - Nanowire - L929	54
4.2.10 Viability Graph - Nanowire - L929	55
4.2.11 Viability Graph - Graphene - L929	56
4.2.12 Viability Graph - Nanotubes - L929	57
4.2.13 OD590 - Nanoclay - L929	59
4.2.14 OD590 - Fullerene - L929	59
4.2.15 Viability Graph - Nanoclay - L929	60
4.2.16 Viability Graph - Fullerene - L929	61
5. CONCLUSIONS	63
6. FUTURE WORK	65
REFERENCES	67

LIST OF TABLES

TABLE	PAGE
3.1 Amount of materials and medium used for testing.....	36
3.2 Table showing the sample solution, SDS and the medium in a 96 well plate.....	40
4.1 OD readings from the preliminary tests of pristine 100 ply Carbon nanowire.....	43
4.2 Table showing OD 590 readings for carbon nanowire, graphene, and carbon nanotube.....	47
4.3 Table showing the OD 590 readings of pristine 100ply Carbon nanowire, graphene, and carbon nanotubes on L929 cells.....	53
4.4 Table showing the OD 590 readings of pristine 100ply Carbon nanowire, graphene, carbon nanotubes, fullerene and nanoclay on L929 cells.....	58

LIST OF FIGURES

FIGURE	PAGE
2.1 Carbon nanotubes attached to a thin metal wire.....	4
2.2 Computerized image of multi-walled Carbon Nanotube.....	5
2.3 TEM images of multi-walled (a and c) and double walled (b) carbon nanotube.....	6
2.4 Armchair, Zig-zag and Chiral arrangements of Carbon nanotube.....	6
2.5 Graphene linkage.....	9
2.6 Scanning electron microscopy (SEM) image of the cross-section of Highly Reduced Graphene Oxide (HRG) 'paper' material.....	9
2.7 Geometrical shapes built onto a 6, 6 ring junction of C ₆₀	10
2.8 HRTEM (High Resolution Transmission electron Microscopy) image of pure C ₆₀ sample.....	10
2.9 (a) Schematic of nm-thick montmorillonite clay aluminosilicate layers. (b) TEM micrograph of 2% Nanoclay, Nanomer [®] I.34TCN — Nylon 6 nanocomposite showing complete dispersion of clay layers into distinct plate-like nanoparticle.....	12
2.10 Cell undergoing necrosis.....	13
2.11 Cells undergoing Apoptosis.....	14
2.12 Cytotoxicity Test Systems.....	14
2.13 Chemical Structure of Trypan Blue.....	15
2.14 HIV-1 MN Trypan Blue staining.....	15
2.15 Chemical Structure of Sulforhodamine B.....	17
2.16 Photomicrographs of cells before and after wounding.....	18
2.17 Figure showing cell colonies that have grown after the assay.....	19
2.18 Chemical reduction of WST-1 to Formazan by cellular dehydrogenases.....	19
2.19 Picture of a spectrophotometer which is used for colorimetric assay during MTT.....	22
2.20 A flowchart showing the degradation Kinetics via Respiratory route.....	24
2.21 Flow chart explaining the mode of transport of nanomaterials within a human body....	29

LIST OF FIGURES (continued)

FIGURE	PAGE
3.1(a) Microscopic image of cultured 3T3 cells at x10 magnification.	34
3.1(b) Microscopic image of cultured L929 cells at x10 magnification.	35
3.2 Representation of Neubauer slide.	38
4.1 Graph showing Viability vs Sample Dilution for pristine 100ply Carbon Nanowire on 3T3.	45
4.2 (a) SEM image of 100 ply pristine Carbon nanowire.	45
4.2 (b) SEM and TEM images of Graphene powder/flakes.	46
4.2 (c) SEM image of Multiwall Carbon Nanotubes.	46
4.2 (d) 3-D model of C60 Fullerene.	46
4.2 (e) SEM image of Nanoclay.	46
4.3 Graph showing the Viability vs Sample Dilution results of Carbon Nanowire on 3T3 cells.	49
4.4 Graph showing the Viability vs Sample dilution of Graphene on 3T3 cells.	50
4.5 Graph showing Viability vs Sample Dilution of Carbon Nanotubes on 3T3 cells.	51
4.6 Image of L929 cells in medium (DMEM).	52
4.7 (a) Image of L929 cells in SDS in 50% SDS (1:1 ratio). (b) Image of L929 cells in SDS in 33.3% SDS (1:2 ratio). (c) Image of L929 cells in SDS in 20% SDS (1:4 ratio). (d) Image of L929 cells in SDS in 11.1% SDS (1:8 ratio).	52
4.8 Graph showing the Viability vs Sample Dilution of 100Ply Carbon Nanowire on L929 cells.	55
4.9 Graph showing the Viability vs Sample Dilution of Graphene on L929 cells.	56
4.10 Graph showing the Viability vs Sample Dilution of Carbon Nanotubes on L929 cells.	56
4.11 Graph showing the Viability vs Sample Dilution of Nanoclay on L929 cells.	60
4.12 Graph showing the Viability vs Sample Dilution of fullerene on L929 cells.	60

LIST OF ABBREVIATIONS

AB	Alamar Blue
AK	Adenylate Kinase
CB	Coomassie Brilliant
CNT	Carbon Nanotube
CVDE	Crystal Violet Dye Elution
DMEM	Dulbecco's Modified Eagle Medium
DNA	Deoxyribonucleic Acid
DRG	Dorsal Root Ganglia
ECIS	Electric Cell-substrate Impedance Sensing
EPA	Environment Protection Agency
GLU	Glucose
GO	Graphene Oxide
GS	Graphene Sheets
IL-8	Interleukin-8
LDH	Lactate Dehydrogenase
MTT	(Di) - Methyl - Thiazol (Diphenyl) - Tetrazolium
MWCNT	Multi Walled Carbon Nanotube
NASA	National Aviation and Space Administration
NMSP	Nanoscale Materials Stewardship Program
NR	Neutral Red
OD590	Optical Density at 590nm
PAC	Phosphatase Acid
PBS	Phosphate Buffer Saline

LIST OF ABBREVIATIONS (continued)

ROS	Reactive Oxygen Species
SDS	Sodium Dodecyl Sulfate
SEM	Scanning Electron Microscope
SNUN	Significant New Use Notice
SPC	Spinal Cord
SRB	Sulforhodamine B
SWCNT	Single Walled Carbon Nanotube
TEM	Transmission Electron Microscope
TSCA	Toxic Substances Control Act
WST	Water Soluble Tetrazolium

CHAPTER 1

INTRODUCTION

1.1 Background

In the recent years, a lot of engineered nanomaterials are fabricated and investigated for their applications. At the nanometer scale, certain materials exhibit new properties which are otherwise not exhibited at the macro scale. For example, materials those are not reactive at macro scale become reactive at the nanoscale largely because of their greatly increased surface area. Some materials that do not conduct electricity or are fragile become excellent conductors and extremely strong when made small enough. At that scale they also become capable to enter human cells and trigger chemical reactions in soil, and thus interfere with biological and ecological processes. Carbon nanowires are a one-dimensional array of carbon atoms which are threaded through carbon nanotube [1]. They have excellent mechanical properties and fairly good electrical properties. When functionalized, their properties improve exceptionally and can be used in bio sensors, implant strengthening, high performance composites etc [1]. Apart from carbon nanowires, other materials like fullerene, carbon nanotubes and nanoclay etc also have potential to be used in medical fields and composite enhancement, amongst other uses [2]. Nanotechnology applications are coming to market at a very fast pace. The worldwide nano product market is estimated to reach \$1 trillion dollars by 2015 (Roco, 2005). About \$10 billion dollars were spent on nanotechnology research and development alone (Holman et al., 2006) [3]. Hand-in-hand with nanotechnology's promise to deliver materials with unique and useful properties, there also comes a big challenge of public concern over their environmental and health effects [3].

1.2 Motivation

Biosafety of nanomaterials has caused increased attention from governments and scientific communities [3]. A lot of investigation has been carried out, individually, on carbon

nanotubes for their effects on the cells, animals and environment, and evaluated for their biosafety. There is some evidence that engineered nanoparticles can have adverse effects on the health. [3]. Graphene oxides are known to exhibit dose-dependent toxicity to cells and animals, such as inducing cell apoptosis and lung granuloma formation, which is also a form of cancer [2]. In spite of the increased research work on bio compatibility of nanomaterials many materials are yet to be explored.

Till now, not much data is available about cytotoxicity studies on nanowires, fullerene or nanoclay. Furthermore, there is almost no study available which compares the toxicity level of these nanomaterials. Comparative studies on the cytotoxicity helps to efficiently apply these materials in both medical and non-medical fields.

1.3 Goal

This thesis will measure and compare the cytotoxicity of carbon nanotubes, fullerene, nanoclay, graphene and pristine 100 ply carbon nanowires by in vitro tests on human (L929) and mice (3T3) fibroblast cells. Based on the result, further application-based analysis will be done. Special emphasis will be laid on carbon nanowires because of their high potential in the future applications [4].

CHAPTER 2

LITERATURE REVIEW

2.1 Carbon Nanowires

Carbon nanowires are strings of carbon atoms or carbon nanotubes (fig. 2.1) [6], which are threaded together in a single dimension. It was first produced by Yosinori Ando and his colleagues at Nagoya University (Japan) amid a welter of nanotube whiskers by shooting an electrical arc between two carbon electrodes in helium atmosphere. They have large aspect ratios which are in the scale of 1000 or more. According to physics laws the conductivity of a nanowire will be much less than that of the corresponding bulk material. This is because there will be scattering from the wire boundaries [6,7]. The effect of scattering will be very significant whenever the wire width is very low i.e. in this case, below the free electron mean free path of the bulk material. One of the other peculiar properties they show are nanowire conductivity is strongly influenced by edge effects. This effect comes from atoms that lay at the nanowire surface and are not fully bonded to neighboring atoms [6,7,8]. One dimensional nanostructures can be used for both efficient transport of electrons and optical excitation, and these two factors make them critical to the function and integration of nanoscale devices.

2.1.1 Applications of Carbon Nanowires

The carbon nanowires have numerous applications and some of them are listed below [9, 10]:

- They can be used in active electronic elements after doping
- Photon ballistic waveguides
- Transparent electrodes for flexible flat-screen displays
- Due to their high aspect ratio, nanowires are also uniquely suited to dielectrophoretic

- Due to their high Young's moduli, their use in mechanically enhancing composites is also being investigated
- By adding tribological additives characteristics and reliability of electronic transducers and actuators can be improved
- Biosensors



Figure 2.1: Carbon nanotubes attached to a thin metal wire [10].

2.2 Carbon Nanotubes

A Carbon nanotube is a tube-shaped material (fig. 2.2), made out of carbon with a diameter in the nanometer scale (fig 2.3), i.e. <1 nm up to 50 nm [11]. Their lengths are typically several microns, but recent advancements have made the nanotubes much longer, and measured in centimetres [11].

It is more or less a graphite layer rolled-up with a continuous unbroken hexagonal mesh with the carbon molecules at the apexes of the hexagons.

Carbon Nanotubes have multiple structures, differing in length, thickness, the type of helicity (fig. 2.4) and number of layers. Although they are essentially formed from the same graphite sheet, their characteristics differ depending on these variations, especially, electrical properties [13].

2.2.1 Applications of Carbon Nanotubes

They have several applications but most of which is still under research. The applications include the following [12,13]:

- Electronics (wires, transistors, switches, interconnects, memory storage devices)
- Opto-electronics (light emitting diodes, lasers)
- Sensors
- Field emission Devices (displays, scanning electron probes, microscopes)
- Batteries/fuel cells
- Fibres/ reinforced composites
- Medicine/biology (fluorescent markers for cancer treatment, biological labels, drug delivery carriers)
- Catalysis
- Gas storage

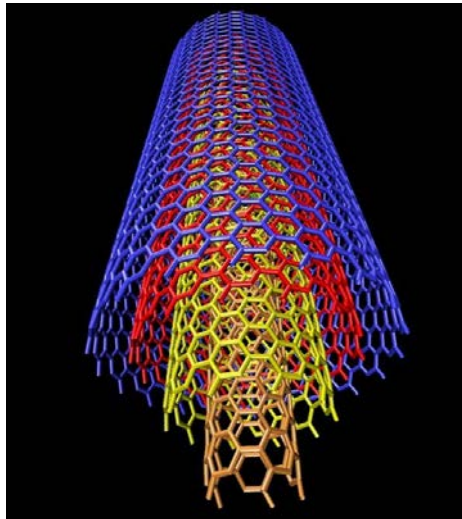


Figure 2.2: Computerized image of multi-walled carbon nanotube[13].

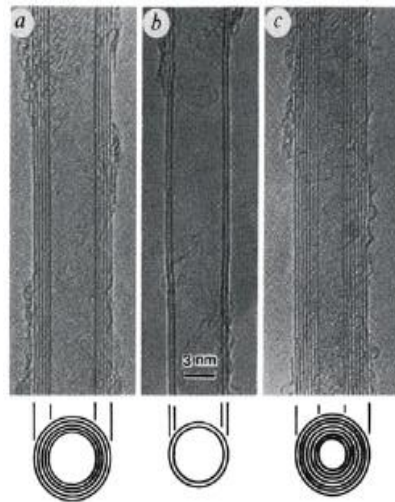


Figure 2.3: TEM images of multi-walled (a and c) and double walled (b) carbon nanotube [4].

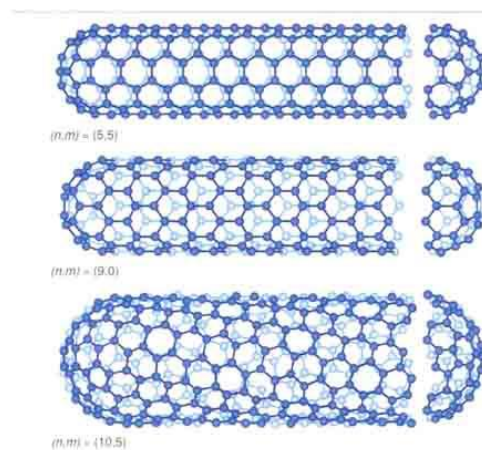


Figure 2.4 Armchair, Zig-zag and Chiral arrangements of carbon nanotube [13].

Another important property of nanotubes is that they can easily penetrate membranes such as cell walls. Their long and narrow shape makes them look like miniature needles which enable them to function like a needle at the cellular level. Medical researchers are using this property by attaching molecules that are attracted to cancer cells to nanotubes to deliver drugs directly to diseased cells [4].

Also, electrical resistance of the nanotube changes significantly when other molecules attach themselves to the carbon atoms. Researchers are using this property to develop highly

sensitive sensors that can detect chemical vapours such as carbon monoxide or biological molecules at a nano-level [2].

Nanotubes that are bound to an antibody produced by chickens have been shown to be useful in lab tests to destroy breast cancer tumors. The antibody that carries those nanotubes is attracted to proteins produced by a one type of breast cancer cell. The nanotubes are then used to absorb the light from an infrared laser which incinerates the nanotubes and subsequently the tumor cells [1].

Researchers at NASA are developing a carbon nanotube based composite that bends when a voltage is applied to it. Only electrical voltage will be required to change the shape (morphing) of aircraft wings and other structures [2,4].

Researchers have found that carbon nanotubes can also be used to fill the voids that occur in conventional concrete. Voids allow water to penetrate into concrete, resulting in the formation of cracks. Nanotubes can be used to stop the cracks from forming and thus increasing the life of the concrete substantially [4].

Lightweight windmill blades can be made with an epoxy containing carbon nanotubes. The increase in the strength and reduction in the weight provided by the use of these nanotube filled epoxy, allows longer windmill blades to be used and in turn, increasing the amount of electricity generated by each windmill [4].

By using carbon nanotubes as the pores in reverse osmosis membranes the power needed to run reverse osmosis desalination plants can be decreased. This is because water molecules pass through carbon nanotubes more easily than through other types of nanopores since their inner walls are much smoother than other types of nanopores [1].

Inexpensive nanotube based sensor can be used in detection of bacteria in drinking water.

Antibodies sensitive to that particular bacteria bind to the nanotubes, these are then deposited onto a paper strip [3].

Several investigations in the past have demonstrated that single-wall carbon nanotubes (SWCNTs) present a noticeable cytotoxicity to human and animal cells while multiwall carbon nanotubes (MWCNTs) not only show a more moderate toxicity than SWCNTs, but also sometimes act as suitable sites for proliferation of bacteria [4].

2.3 Graphene

Graphene is a single-atom-thick sheet of sp²-bonded carbon atoms in a closely packed honeycomb two-dimensional lattice as seen in figure 2.5 and 2.6 [13]. It is a unique form of carbon in which the atoms are arranged in a hexagon. It is the thinnest and the strongest material in the world. It is one of the most fascinating nanostructures having unique physical, chemical, electrical, and mechanical properties which qualify it as a promising nanomaterial in areas such as high-energy physics, material science and a wide range of technological applications, such as bioelectronics and biosensing [13]. It can conduct electricity better than copper can, and it is able to transfer heat better than any other material. On top of that, it is transparent as well. Some of their properties are similar to the properties of carbon nanotubes (CNTs).

2.3.1 Applications of Graphene

The scientists believe that it could be used for lots of applications such as [14]:

- Transistors,
- Transparent conductors
- Surfactants
- Polymer reinforcement
- Biodevices.

Recently, similar to carbon nanotubes (CNTs), biological applications of graphene sheets (GS) and graphene oxide (GO) have attracted attention in the scientific community based on their great potential for the following [14, 15]:

- Bacterial inhibition
- Drug delivery
- Photo-thermal therapy

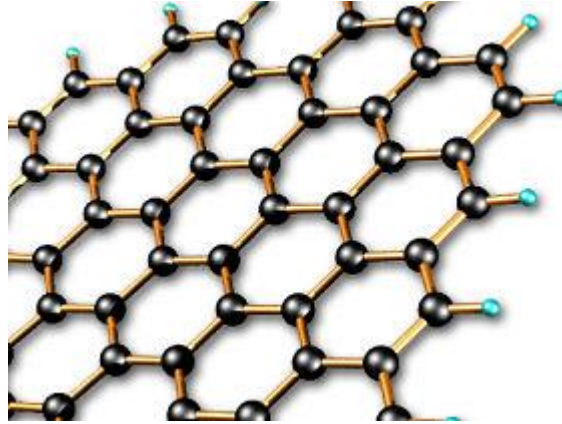


Figure 2.5: Graphene linkage [14]

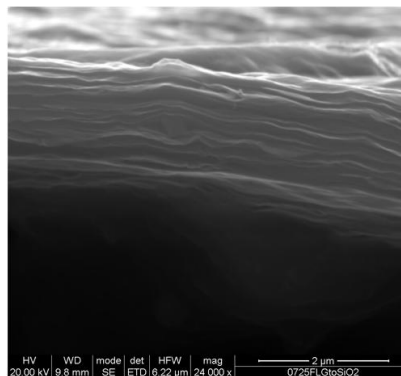


Figure 2.6: Scanning electron microscopy (SEM) image of the cross-section of Highly Reduced Graphene Oxide (HRG) 'paper' material [15]

2.4 Fullerene

Fullerene is also known as C₆₀ because it is made of 60 carbon atoms. The C₆₀ surface contains 20 hexagons and 12 pentagons in which, all the rings are fused and all the double bonds are conjugated [16]. There are various shapes into which they can be built as seen in figure 2.7, such as [17]:

- Open
- Three-membered ring

- Four-membered ring
- Five-membered ring and
- Six-membered ring

Figure 2.8 shows a High Resolution Transmission Electron Microscopic image of pure C 60 sample.

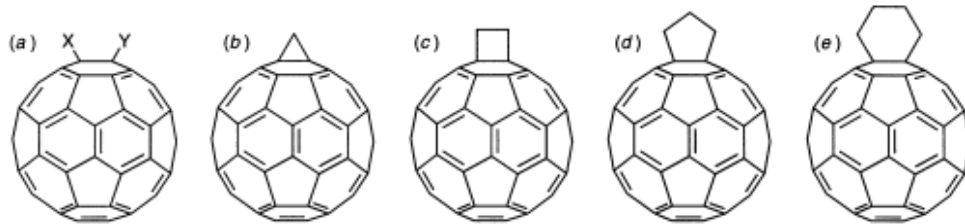


Figure: 2.7: Geometrical shapes built onto a 6, 6 ring junction of C60 [17]

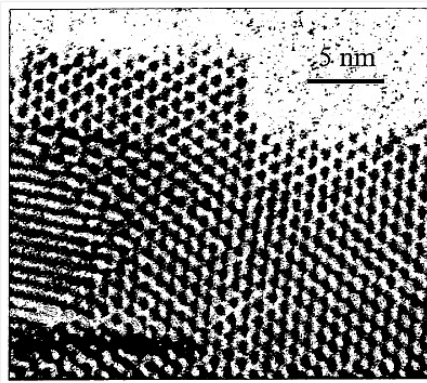


Figure 2.8: HRTEM image of pure C60 sample [16].

2.4.1 Applications of Fullerene

Fullerene due to its exotic properties can have a wide variety of applications most of which are still under research. These have been discussed below:

- In materials science, the rich electronic and electrochemical behaviour of C 60 generated great expectations. However, the difficult processibility of the fullerenes has represented a major problem in the hectic search for practical applications. C 60 is insoluble or only sparingly soluble in most solvents and aggregates very easily. The major areas of applications (but still too expensive) inorganic electronics and bioscience include the following [16,17]:

- Electrical conductivity of alkali-doped C₆₀: K₂C₆₀ is an insulator but K₃C₆₀ becomes superconductor at 18K and Rb₃C₆₀ becomes a superconductor at 30K.
- Catalysts for hydrocarbon upgrading: Conversion of heavy oils, methane into higher hydrocarbons.
- Pharmaceuticals: Derivatives of C₆₀ are highly hydrophobic and antioxidant (they soak cell-damaging free radicals) and hence can be used as protease inhibitor.
- Battery anodes
- Proton transport membranes
- Buckyfilms
- Sharper scanning microscope
- Sporting goods like badminton racquets with fullerenes in the polymer matrix composite
- Cosmetics, such as the Vitamin C₆₀ skin creams

The ability to add an electron and then remove it with almost no energy cost can be applied in a primary biological application: as antioxidants. Certain water-soluble fullerenes are capable of catalytically removing potentially harmful oxidant species, acting as a synthetic analog to naturally-occurring superoxide dismutase. Their antioxidant behaviour has extended in the lifespan of geriatric mice, and has also improved their advanced age cognition. Due to this, water-soluble fullerenes (such as C₆₀ Pyrrolidine tris-acid) are explored for applications in therapies against a variety of degenerative conditions involving an excess of reactive oxygen species. Fullerenes are also being developed for drug delivery applications. They have a rich and well-documented organic chemistry, and many versatile routes have been developed for the formation of covalent bonds to fullerenes. Various therapeutic agents have been covalently linked to C₆₀ and used as drug delivery agents.

2.5 Nanoclay

Nanoclays are clay minerals which are ground and optimized for use in clay nano composites. They are multi-functional material systems whose properties can be selectively enhanced for a particular application [18]. Polymer-clay nano-composites are well-researched class of such materials (fig 2.9). Nanoclays are a broad class of naturally occurring inorganic minerals, out of which plate-like montmorillonite is the most commonly used in materials applications. Montmorillonite consists of ~ 1 nm thick aluminosilicate layers surface-substituted with metal cations and stacked in ~ 10 μm -sized multilayer stacks which can be dispersed in a polymer matrix to form polymer-clay nanocomposite [18]. Within the nanocomposite, individual nm-thick clay layers are separated to form plate-like nanoparticles with very high ($\text{nm} \times \mu\text{m}$) aspect ratio. Even at low loading (a few weight %), the entire composite consists of interfacial polymer, with majority of polymer chains residing in close contact with the clay surface which can alter the properties of a nanocomposite [18].

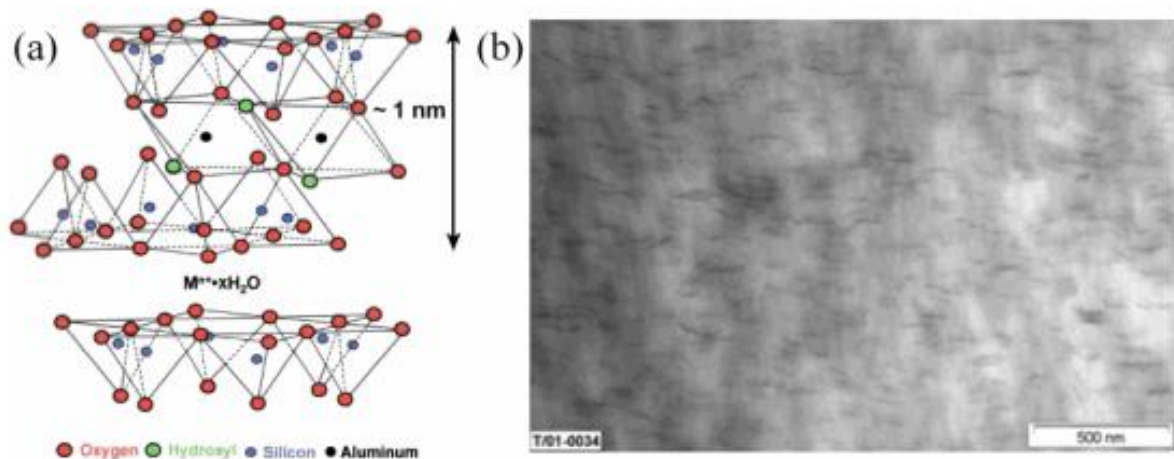


Figure 2.9: (a) Schematic of nm-thick montmorillonite clay aluminosilicate layers. (b) TEM micrograph of 2% Nanoclay, Nanomer[®] I.34TCN — Nylon 6 nanocomposite showing complete dispersion of clay layers into distinct plate-like nanoparticles [18].

2.6 Cytotoxicity

According to the medical dictionary by Farlex it means the degree to which an agent possesses a specific destructive action on certain cells. Any substance or materials capable of killing or destroying live healthy cells which may include snake venom or animal lymphocytes are called cytotoxic [19].

Treating cells with the cytotoxic compound can result in a variety of cell deaths as given below:

- 1) Necrosis- During this process the cells lose membrane integrity and die rapidly as a result of cell lysis. Cells undergoing necrosis typically exhibit rapid swelling, lose membrane integrity, shut down metabolism and release their contents out into the environment as shown in figure 2.10. Cells that undergo rapid necrosis in vitro do not have sufficient time or energy to activate apoptotic machinery and do not express apoptotic markers [19].



Figure 2.10: Cell undergoing necrosis [19]

- 2) Apoptosis – During Apoptosis a change in refractive index first takes place. This is followed by cytoplasmic shrinkage and nuclear condensation. The cell membrane starts showing blebs or spikes which are protusions of cell membrane. Depending on the type of the cell, these blebs separate from the dying cell and form apoptotic bodies. These cells also cease to maintain phospholipid asymmetry in the cell membrane. The mitochondrial outer membrane also undergoes changes that include loss of its electrochemical gradient. Then adjacent cells or macrophages phagocytose

apoptotic bodies and the dying cell. There is no inflammatory response like in the previous case. The process is depicted in figure 2.11 [19].

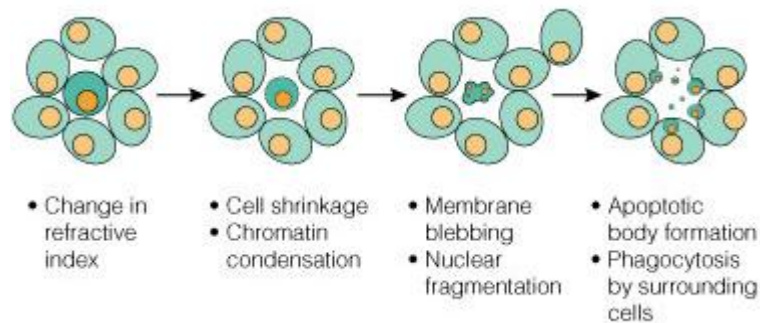


Figure 2.11: Cells undergoing Apoptosis [19]

Morphology changes during apoptosis: the cell membrane begins to show blebs or spikes, depending in cell type. Eventually these separate from the dying cell and from the apoptotic bodies that are phagocytosed by neighbouring cells.

The diagram below (fig 2.12) shows the region within a cell, where a particular cytotoxicity test would act up. The test and their effecting area are as follows:

- Membrane integrity (LDHe)
- Metabolic activity (GLU)
- Respiratory chain activity (XTT/MTT)
- Total protein synthesis (SRB)/below mentioned
- DNA content and (CVDE) and
- Lysosomal activity(PAC, NR)

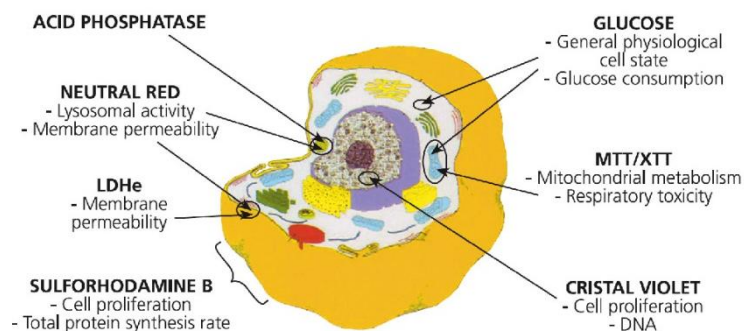


Figure 2.12: Cytotoxicity Test Systems [20]

2.7 Types of Cytotoxic Assays

2.7.1 Trypan Blue or Propidium Iodide

It is a method of cytotoxicity testing in which dead cells stain blue while the live cells do not react with trypan blue (fig 2.14)[21]. These dead cells can be seen under a microscope. The reactivity of trypan blue is based on the fact that the chromophore is negatively charged and does not interact with the cell unless the membrane is damaged [21, 22]. When the membrane is damaged the negatively charged chromophore reacts with trypan blue and stains itself. Therefore, all the cells which exclude the dye are viable. This method cannot distinguish necrotic vs. apoptotic cells [23].

Formula : $C_{34}H_{24}N_6Na_4O_{14}S_4$

Tetrasodium 3,3'-[(3,3'-dimethyl[1,1'-biphenyl]-4,4'-diyl)bis(azo)]bis[5-amino-4-hydroxynaphthalene-2,7-disulphonate] – (Fig 2.13) [24,25]

Molecular Weight: 960.81 g/mol [25]

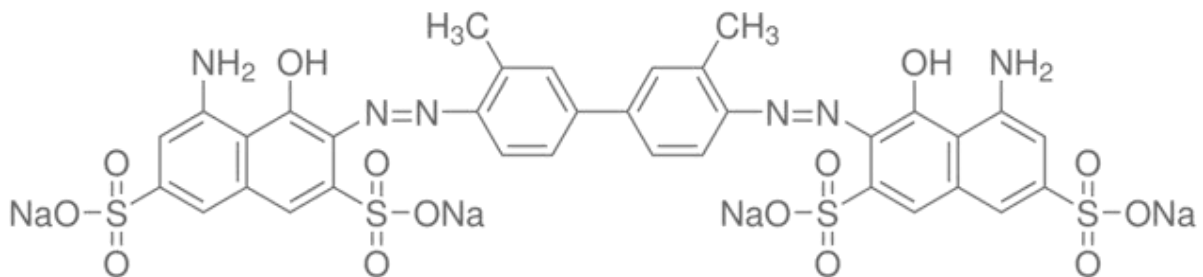


Figure 2.13: Chemical Structure of Trypan Blue [24]

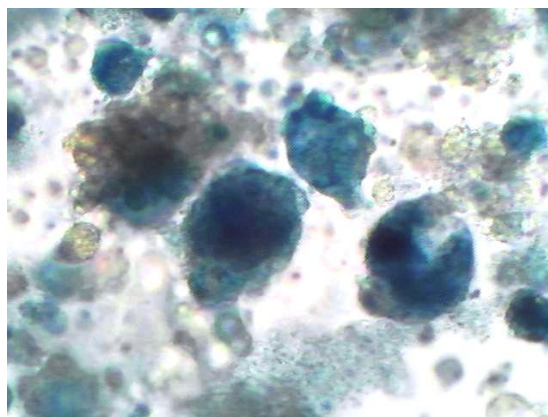


Fig 2.14: HIV-1 MN Trypan Blue staining [25]

2.7.2 Lactate Dehydrogenase (LDH)

Lactate dehydrogenase also called lactic acid dehydrogenase is an enzyme that is found in almost all body tissues. It plays an important role in cellular respiration, where in, the glucose (sugar) from food is converted into usable form of energy for our cells [26]. Although LDH is abundant in tissue cells, their levels are low in the blood. Whenever tissues are damaged by injury or by disease, more LDH is released into the bloodstream. Conditions like liver disease, heart attack, anemia, muscle trauma, bone fractures, cancers, and infections such as meningitis, encephalitis, and HIV increase the amount of LDH in the blood stream. Currently, LDH is mainly used as a general indicator of the existence and severity of acute or chronic tissue damage. Earlier it was used to help diagnose and monitor a heart attack, but the Troponin test has largely replaced LDH in this role. LDH isoenzymes may also be used in differential diagnosis to help determine which organs are likely to be involved [26, 27].

2.7.3 Sulforhodamine B (SRB) Assay

The SRB assay was developed by Skehan and colleagues to measure cytotoxicity and cell proliferation induced by drug [28]. It is extensively used in large-scale drug-screening applications. Its principle is based on the ability of the protein dye sulforhodamine B (fig 2.15) to bind electrostatically to amino acid residues of trichloroacetic acid-fixed cells. Under these mild acidic conditions it binds and under mild basic conditions it is extracted from cells and solubilised. Its sensitivity is comparable to several fluorescence assays and superior to that of Lowry or Bradford [29]. The signal-to-noise ratio of this assay is favourable and the resolution is 1000-2000 cells/well. The SRB assay is also used for cell density determination, based on the measurement of cellular protein content [28, 29, 30].

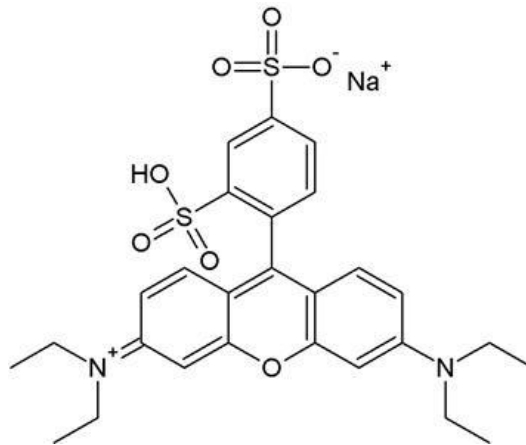


Figure 2.15: Chemical Structure of Sulforhodamine B [30]

2.7.4 Electric Cell-substrate Impedance Sensing (ECIS)

In ECIS technology the change in impedance of a current flow through the cell culture medium is measured. As cells grow on the electrode they constrict current flow altering the impedance. The measurement is in a non-invasive manner, visualizing the effects like cell attachment, cell-cell contacts or cell proliferation [34]. ECIS measures the complex impedance of small 250-micrometer diameter electrodes used as substrates for cell growth. An improved technology called ECIS Z θ (Z theta), which is a turnkey system that provides an advanced, automated, non-invasive way to monitor cell behaviour in real-time [34]. The ECIS Z θ reliably monitors up to 8, 16 or 96 tissue culture wells and interprets the complex impedance as both resistance and capacitance. By using a mathematical model the system can report time course changes in the barrier function (permeability) of confluent cell layers as well as membrane capacitance. ECIS is not only limited to these layers and has proved particularly useful for studying endothelial cell layers continuously. The ECIS can be used to control the following factors which also includes

Wound/Electroporate Option (fig 2.18) [35]:

- User specified wound time, current and frequency
- Delayed wounding during data collection

Flow Option [35]:

- Ability to measure under dynamic flow conditions
- Control pump flow rates from the ECIS software
- Control up to 8 pumps simultaneously
- Ability to program pulsed flow mode
- User controlled shear stress

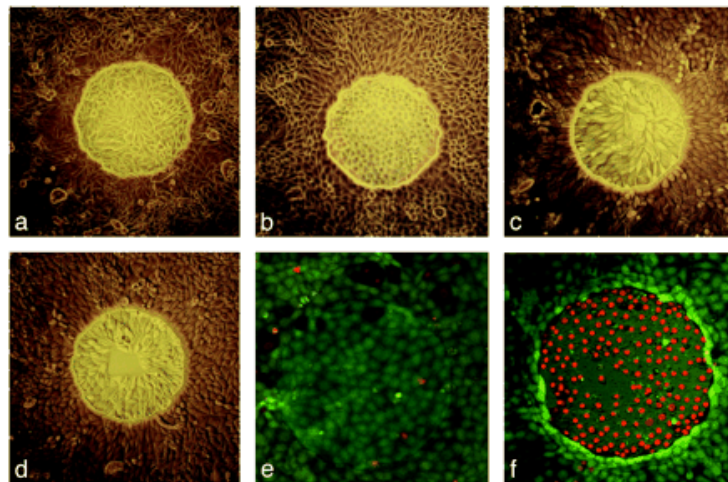


Figure 2.16: Photomicrographs of cells before and after wounding [35].

2.7.5 Clonogenic Assay

Clonogenic assay or colony formation assay is an *in vitro* assay based on the ability of a single cell to grow into a colony. A colony is defined to consist of at least 50 cells. The assay essentially tests every cell in the population for its ability to undergo unrestricted division. Clonogenic assay is used to determine cell reproductive death after treatment with ionizing radiation, but can also be used to determine cytotoxicity [33]. Only few seeded cells retain the capacity to produce colonies. Before or after treatment, cells are seeded out in appropriate dilutions to form colonies (fig 2.17) within 1–3 weeks. Colonies are fixed using glutaraldehyde (6.0% v/v), stained with crystal violet (0.5% w/v) and counted using a stereomicroscope [34].

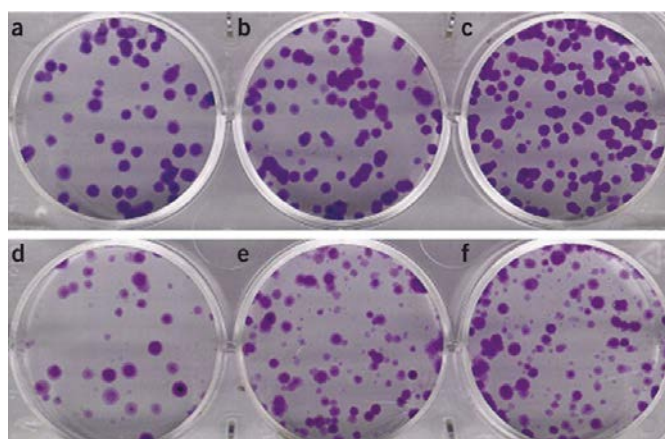


Figure 2.17: Figure showing cell colonies that have grown after the assay [33].

2.7.6 Water Soluble Tetrazolium (WST) Assay

This assay is based on the cleavage of the tetrazolium salt to form formazan (fig 2.16). This is done by cellular mitochondrial dehydrogenases [31]. Expansion of viable cell numbers results in an increase in the overall activity of the mitochondrial dehydrogenases in the sample which in turn leads to an increase in formazan dye metabolism. This formazan dye produced by the viable cells is measured at an absorbance of 440 nm using a standard multiwell spectrophotometer. The assay is used to determine cell proliferation in response to interactions with drugs, growth factors, cytokines, mitogens, and nutrients. This method is simple and does not require cell washing, harvesting, or any solubilization steps [31, 32].

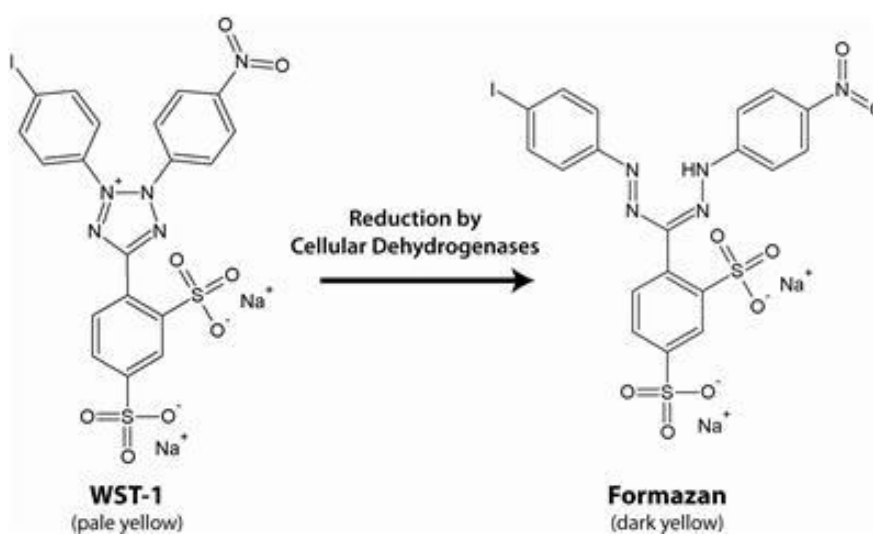


Figure 2.18: Chemical reduction of WST-1 to Formazan by cellular dehydrogenases [32]

2.7.7 MTT or MTS Assay

It is a type of WST colorimetric assay in which (3-(4, 5-Dimethylthiazol-2-yl)-2, 5-diphenyltetrazolium bromide is used as the reacting agent. In MTT assay this yellow tetrazolium salt (MTT) is reduced, in the presence of metabolically active cells, to form insoluble purple formazan crystals [36]. These crystals are solubilized by the addition of a detergent. The colour can then be quantified by spectrophotometric means. For each cell type a linear relationship between cell number and absorbance is established which enables accurate, straightforward quantification of any change in proliferation. Among the applications for this method are drug sensitivity, cytotoxicity, response to growth factors, cell activation etc. The special features of MTT assay are as given below [37, 38] :

- Proven technology- The utility of the MTT method has been well documented in the literature for various applications.
- Accurate measurements- The spectrophotometric procedure can detect even slight changes in cell metabolism, thereby making it much more sensitive than trypan blue assay.
- Safer reagents- There is no need for special storage or manipulation of any kind of radioactive by-products.
- Easy to use- The procedure is relatively simple and uses equipment which is available in most labs.
- Rapid processing- The assays are run in a 96 (12x8) well plate and read with a microtitre plate reader, allowing high-throughput handling of samples.
- Convenient storage - The reagents are stable for 18 months when stored under refrigeration in the dark.

2.8 Optical Density

A transmissive material absorbs some light falling on it, reflect some and pass the remainder. The fraction of light that is passed is called transmittance [38]. When the intensity of light incident on a translucent material is denoted as I_0 , and the intensity of that which passes through is denoted by I , the transmittance T is defined by

$$T = I/I_0$$

Transmittance takes on values between 0 and 1. Nearly all the transmittance values are less than 1 and in many instances provide decimals that are difficult to correlate with the visual impressions. For example, the transmittance of 0.0001 has very little correlation with a visual interpretation of what that means, since the eye tends to react to radians more in a logarithmic manner. Because of this, the negative logarithm of transmittance is used. This is known as optical density (D) [38, 39].

$$D = -\log_{10}(T)$$

Density reflects the values of the incident light that fails to pass through the material. The density takes on values from zero to infinity. Spectroscopy is a method used to study the absorption and emission of light and Spectrophotometry is the quantitative measurement of the reflection or transmission properties of a material as a function of wavelength. Below given in a figure (fig 2.19) of a spectrophotometer that is usually used for MTT cytotoxicity testing [39].

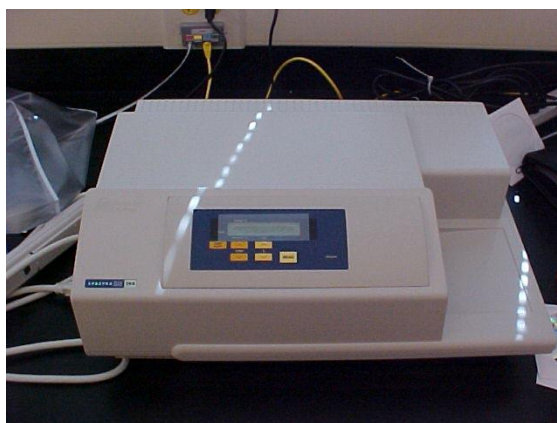


Figure 2.19: Picture of a spectrophotometer which is used for colorimetric assay during MTT.

2.9 Harmful Effects of Toxic Nanomaterials

Among diseases associated with nanoparticles are asthma, bronchitis, lung cancer, neurodegenerative diseases (such as Parkinson's and Alzheimer's diseases), Crohn's disease, colon cancer. Nanoparticles that enter the circulatory system are related to occurrence of arteriosclerosis, and blood clots, arrhythmia, heart diseases, and ultimately cardiac death. The researches conducted on various nanomaterials have been discussed in the subsequent sections. Their effects on lungs cells, blood cells, fetal cells, skin cells, neural cells etc have been discussed in detail [64-71].

2.9.1 Respiratory Cytotoxicity

When respiratory toxicity of multi wall carbon nanotubes were studied oxidative stress, prominent pulmonary inflammation, apoptosis in different cell types, and induction of cytotoxic effects were seen. The study conducted by Muller et.al (2005) [40] suggests that ground CNT's are more harmful and can reach the alveolar spaces and induce the formation of parenchymal granulomas. Agglomerates of intact CNTs remained entrapped in the largest airway, whereas ground nanotubes were much better dispersed in the lung tissue. These tissues Upon reaching the respiratory tract, cause pulmonary inflammation, pulmonary fibrosis, induced accumulation of neutrophils and eosinophils, mechanical blockage, and increase in various cytotoxicity/inflammatory markers in the lungs. Further the study by

Smart et.al (2006) [41] suggests that high-purity smaller size carbon black (15nm) on pulmonary tissue can cause increased oxidative stress in human type II alveolar epithelial cells and increased murine alveolar macrophage migration in foetal calf serum. Their destructive power is nearly two fold, as compared with high-purity CB of a greater size (260 nm). Stoker et.al (2007) [42] in his in vitro study assessed the health risk of CNTs on the human respiratory system by using co-culture of normal bronchial epithelial cells and normal human fibroblasts. Maria et.al (2008) [43] conducted toxicity evaluation on A549 lung cells using the alamar blue (AB), neutral red (NR) and MTT assays, which evaluated metabolic, lysosomal and mitochondrial activity respectively. In addition, the total protein content of the cells was measured using the coomassie brilliant (CB) blue assay. Supernatants were also assayed for Adenylate Kinase (AK) release and Interleukin 8 (IL-8) and they indicated a loss of cell membrane integrity and an inflammation response respectively. Of the multiple cytotoxicity assays used, the AB assay was found to be the most sensitive and reproducible. Iron-contaminated SWCNT were also reported in other studies to exhibit cytotoxicity in A549 or BEAS-2B cells (Herzog et al., 2007), BEAS-2B cells (Shvedova et al., 2004), and RAW 264.7 cells (Kagan et al., 2006). However, SWCNT samples with low iron contamination were found to be significantly less toxic (Kagan et al., 2006; Herzog et al., 2007). Shvedova et al. (2008a) reported that in vitro exposure of primary mouse alveolar macrophages to SWCNT decreases phagocytosis. Emily et.al conducted studies on 3-D Tissue Engineered Human Lung (fig 2.20). They measured the production of nitric oxide (NO) as an inflammatory marker and mitochondrial activity using MTT (3-(4,5-Dimethylthiazol-2-yl)-2,5-diphenyltetrazolium bromide) assay. Their results indicated that NO production was dramatically increased and cell viability was decreased following exposure to different concentrations of SWCNTs.

2.9.2 Fibroblast and Skin Cytotoxicity

According to the study conducted by Kan et.al (2011) [44] bio compatibility of Graphene oxides on human fibroblast cells was tested using CCK8 assay. According to them, Graphene oxides with dose less than 20 $\mu\text{g/ml}$ did not exhibit toxicity to human fibroblast cells, and the dose of more than 50 $\mu\text{g/ml}$ exhibited obvious cytotoxicity such as decreasing cell adhesion, inducing cell apoptosis, entering into lysosomes, mitochondrion, endoplasm, and cell nucleus.

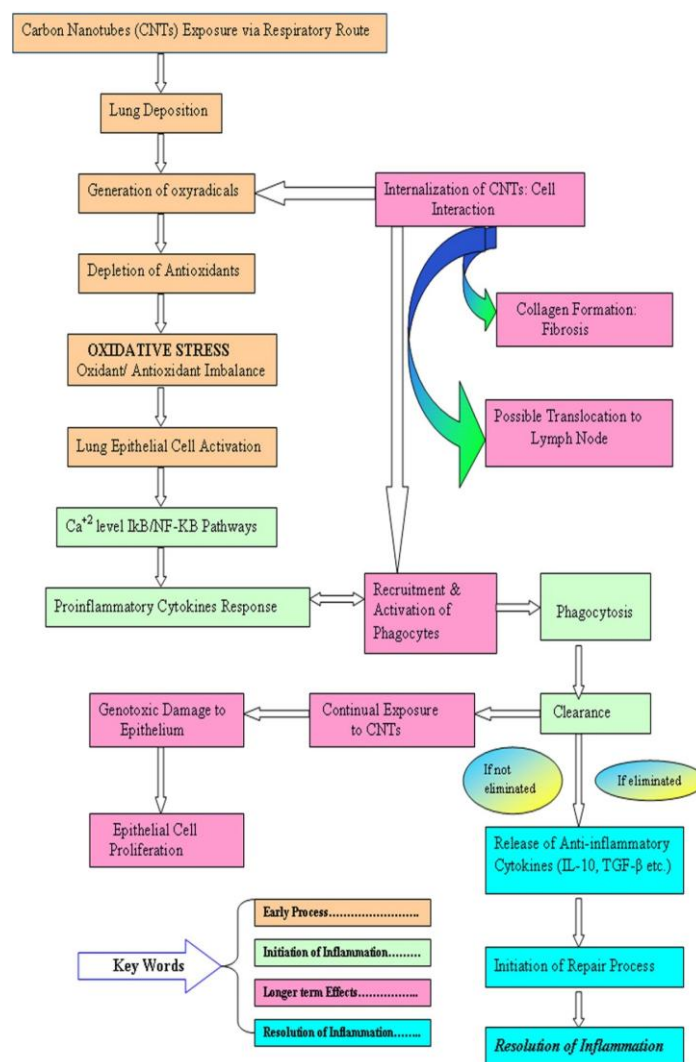


Figure 2.20: A flowchart showing the degradation Kinetics via Respiratory route [43].

Liao et.al (2011) [14] studied the comparison between the effect of graphene and graphene oxide on human erythrocytes and skin fibroblasts. According to them, at the smallest size, graphene oxide showed the greatest hemolytic activity, whereas aggregated graphene sheets

exhibited the lowest hemolytic activity. Coating graphene oxide with chitosan eliminated hemolytic activity. The investigation was done by measuring mitochondrial activity in adherent human skin fibroblasts using WST-8, trypan blue exclusion, and reactive oxygen species assays. The compacted graphene sheets were more damaging to mammalian fibroblasts than the less densely packed graphene oxide. In the study conducted by Furong et.al (2006) [46] the cell survival and attachment assays were evaluated with different concentrations of refined: (i) single-wall carbon nanotubes (SWCNTs), (ii) active carbon, (iii) carbon black, (iv) multi-wall carbon nanotubes, and (v) carbon graphite. They found that SWCNTs induced the strongest cellular apoptosis / necrosis. Refined SWCNTs were more toxic than their unrefined counterpart. Exposure to graphite and carbon materials has been associated with increased incidence of skin diseases, such as carbon fiber dermatitis, hyperkeratosis, and naevi. Amongst the research conducted on human skin cells, effect of Carbon Nanotube on human keratinocyte cells was studied by Shvedova et.al. (2003) [52] After 18 h of exposure to SWCNT, oxidative stress and cellular toxicity were indicated by formation of free radicals, accumulation of peroxidative products, antioxidant depletion, and loss of cell viability. Exposure to SWCNT also resulted in ultrastructural and morphological changes in cultured skin cells. According to this data, dermal exposure to unrefined SWCNT may lead to dermal toxicity due to accelerated oxidative stress in the skin.

2.9.3 Neural Cytotoxicity

Some groups also conducted studies on neural cells. The study conducted by Yongbin et.al (2010) [47] which involved study of the effect of Graphene and Single-Wall Carbon Nanotubes in Neural Phaeochromocytoma PC12 Cells suggest that both G and SWCNT induce cytotoxic effects, and these effects are concentration and shape-dependent. At low concentrations, G induced stronger metabolic activity than SWCNT which reversed at higher concentrations. They used LDH release and apoptosis & reactive oxygen species

measurement. Another study was done by Belyanskaya et.al (2009) on the influences of single-walled CNTs (SWCNTs) on primary cultures derived from chicken embryonic spinal cord (SPC) or dorsal root ganglia (DRG). Hoechst assay was done and it was seen that mixed neuro-glial cultures with up to 30 $\mu\text{g}/\text{mL}$ SWCNTs significantly decreased the overall DNA content. Using a cell-based ELISA they found that SWCNTs reduce the amount of glial cells in both peripheral nervous system (PNS) and central nervous system (CNS). The SWCNT suspensions used in this study induced acute toxic effects in primary cultures.

2.9.4 Cytotoxicity on Human Circulatory System

Massimo et.al (2006) [48] conducted tests on T-lymphocyte using multi-walled carbon nanotubes. A comparison of the toxicity of pristine and oxidized multi-walled carbon nanotubes on human T cells was done and it was found that the latter are more toxic and induce massive loss of cell viability through programmed cell death at doses of 400 $\mu\text{g}/\text{ml}$, which corresponds to approximately 10 million carbon nanotubes per cell. They used Neubauer hemocytometer to measure Cell proliferation. According to Kalbacova et.al (2006) [49] single-walled carbon nanotube (SWCNT) films destroyed the metabolic activity of mesenchymal cells only slightly (about 20%), while carbon fibers led to a much stronger decrease (about 40%). Julie et.al (2008) [50] studied the clastogenic and aneugenic effects of multi-wall carbon nanotubes in epithelial cells. In vivo, micronuclei (MN) were assessed in type II pneumocytes 3 days after a single intra-tracheal administration of MWCNT (0.5 or 2 mg) in rats. A significant and dose-dependent increase in micronucleated pneumocytes after a single administration of MWCNT (a 2-fold increase at the highest dose), was seen. They also found that MWCNT induced both centromere- positive and -negative MN in MCF-7 cells. Paul et.al (2008) [51] conducted near-Infrared Fluorescence Microscopy of Single-Walled Carbon Nanotubes in Phagocytic Cells. Macrophage samples that were incubated in growth media containing suspended single-walled nanotubes showed characteristic nanotube

fluorescence spectra. The fluorescence intensities increased smoothly with incubation time and external nanotube concentration.

According to the test conducted by Guang et.al (2005) [53], the cytotoxicity apparently follows a sequence order on a mass basis: SWNTs > MWNT10 > quartz > C₆₀. SWNTs significantly impaired phagocytosis of AM at the low dose of 0.38 µg/cm², whereas MWNT10 and C₆₀ induced injury only at the high dose of 3.06 µg/cm². MTT cytotoxicity tests on guinea pigs were done and cells exposed to SWNTs of 3.06 µg/cm² died. In general swelling of the endoplasmic reticulum, vacuolar changes, phagosomes, and chromatin condensation at nuclear envelope were seen at 8000 magnification. According to Nicola et.al (2009) who studied the effects of multiwalled carbon nanotubes (MWCNT) on healthy monocytes from human peripheral blood, MWCNT exert a cytotoxic effect on monocytes, inducing cell death and increasing the extent of apoptosis induced by a chemotherapeutic agent.

2.9.5. Toxic effects on DNA

Peterson et.al (2011) [54] reviewed the Reactive Oxygen Species (ROS) toxicity of nanoparticles on the cell nucleus and DNA material. The accumulation of single strand breaks and oxidative induced base lesions can lead to double strand breaks. This type of breakage is considered the most lethal type of oxidative damage to DNA. Large amount of ROS can damage the mitochondrial DNA (mtDNA) which is associated with several clinical syndromes such as neurogenic muscle weakness, ataxia and retinitis pigmentosa, mitochondrial encephalomyopathy lactic acidosis, stroke like episodes, retinitis pigmentosa, cardiac conduction defect and elevated cerebrospinal fluid protein. Apart from ROS effects, certain physicochemical properties of nanoparticles can also induce cytotoxicity. Minchin et al. [55] showed that some nanoparticles cause unfolding of fibrinogen, hence promoting its interaction with the integrin receptor, Mac-1. Activation of this receptor up regulates the NFκB signalling pathway which results in the release of inflammatory cytokines.

2.10 Reasons for Cytotoxicity

Some of the reasons for cytotoxicity, according to the previous research work, have been discussed below: [1, 14, and 19]

- They are nanoparticulate and so have more toxicity than larger sized particles because of better absorbability.
- They are fibre shaped and so might behave like asbestos and other pathogenic fibers, which have toxicity associated due to their needle-like shape.
- They are essentially graphitic and so are almost non biodegradable.
- Toxicity of functionalized CNTs -oxidized nanotubes are usually more toxic than their unmodified counterparts. Oxidized MWCNTs are more highly dispersed in aqueous solution, which provide a higher probability for interaction with cells.
- Certain types of CNTs functionalized with lipids are highly water-soluble, which facilitate their movement through the human body and might also reduce the risk of blockage of vital body organ pathways.

2.11 Mode of Transport of Nanomaterial within a Humanbody

Nanoparticles because of their very small size are capable of entering the human body by inhalation, ingestion, skin penetration or injections, and they have the potential to interact with intracellular structures and macromolecules for long periods of time. Spread of the deposited particles in the respiratory tract takes place by two mechanisms: (1) physical translocation of particles by different mechanisms and (2) chemical clearance processes.

- Oberdorster et al found significant amounts of C13-labeled carbon particles which were 22–30 nm in diameter in the livers of rats as soon as after 6 hours of inhalation exposure.

- Colvin et.al found that inhaled C13-labeled carbon particles reached the olfactory bulb and also the cerebrum and cerebellum. The results suggest that translocation to the brain occurred through the nasal mucosa along with the olfactory nerve.
- Intraperitoneal administration of 50-nm fluorescent magnetic nanoparticles was found to penetrate the blood-brain barrier without causing significant toxicity.

Figure 2.21 is a schematic representation of how spread of nanomaterials occurs through the human body. According to the flowchart nanoparticles usually enter the human body through inhalation. After they pass through the respiratory tract they may enter the neural system or the circulatory system or the lymphatic system. Through these systems they can affect the spleen, heart, kidney, bone marrow or liver. The distribution in the respiratory system is called primary distribution, the one in the nervous, circulatory and lymphatic system is called secondary distribution and the remaining is called tertiary distribution.

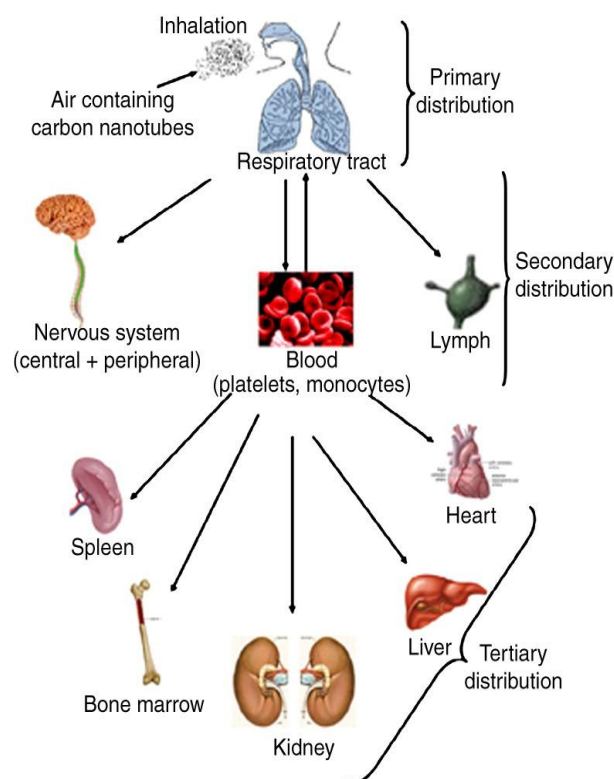


Figure 2.21: Flow chart explaining the mode of transport of nanomaterials within a human body [54].

2.12 Usefulness of Cytotoxicity

According to Yoshinori et.al (2005) [56], who studied the Influence of length on cytotoxicity of multi-walled carbon nanotubes against human acute monocytic leukemia cell line THP-1 in vitro and subcutaneous tissue of rats in vivo, reported that the degree of inflammation around 825-CNTs was stronger than that around 220-CNTs since macrophages could envelop 220-CNTs more readily than 825-CNTs, where the numbers indicates the length in nm of the carbon nanotubes. Another work carried out by Omid et.al (2010) [57], on cytotoxicity of Graphene on bacteria suggested that cell membrane damage of the bacteria caused by direct contact of the bacteria with the extremely sharp edges of the nanowalls was the effective mechanism in the bacterial inactivation. Graphene oxide nanowalls reduced by hydrazine were more toxic to the bacteria than the unreduced graphene oxide nanowalls. They used RNA efflux test and the damaged cell membranes of both Gram-negative E. coli and Gram positive Staphylococcus aureus (S. aureus) bacteria were examined. Also, in vitro tests conducted by Dutta et.al indicate that SWCNT inhibit the ability of RAW264.7 cell to produce cyclooxygenase-2 (COX) in response to the bacterial lipopolysaccharide.

2.13 Protection and Preventive Measures

According to the United States Environment Protection Agency, many nanoscale materials are regarded as "chemical substances" under the Toxic Substances Control Act (TSCA). To ensure proper manufacture and usage of nanomaterials, EPA is pursuing a comprehensive regulatory approach, which includes: Premanufacture notifications; a Significant New Use Rule; an information gathering rule; and a test rule [58].

Pre-manufacture Notifications - TSCA requires manufacturers of new chemical substances to provide specific information to the Agency for review prior to manufacturing chemicals or introducing them into commerce. The Agency has taken a number of actions which are as given below:

- Limiting the uses of the nanoscale materials
- Requiring the use of personal protective equipment, such as impervious gloves and NIOSH approved respirators
- Limiting environmental releases
- Requiring testing to generate health and environmental effects data.

Significant New Use Rule (SNUR) - Under section 5(a)(2) of TSCA a new use rule is being developed to ensure that nanoscale materials receive proper regulatory review.

According to this rule, persons who intend to manufacture, import, or process new nanoscale materials will have to submit a Significant New Use Notice (SNUN) to EPA at least 90 days before commencing that activity. The SNUR would then identify existing uses of nanoscale materials based on information submitted under the Agency's voluntary Nanoscale Materials Stewardship Program (NMSP). The SNUNs would provide the Agency with a basic set of information on nanoscale materials, such as chemical identification, material characterization, physical/chemical properties, commercial uses, production volume, exposure and fate data, and toxicity data according to which the Agency will evaluate the intended uses of these nanoscale [58].

Information Gathering Rule- To ensure a comprehensive understanding of nanoscale materials that are already in commerce, EPA is also developing a proposed rule under TSCA section 8(a) to require the submission of additional information. According to this rule, the persons who manufacture these nanoscale materials should notify EPA of certain information including production volume, methods of manufacture and processing, exposure and release information, and available health and safety data.

Test Rule - Under TSCA section 4 EPA will propose a rule to require testing for certain nanoscale materials materials that are already in commerce, especially the ones that are not already being tested by other Federal and international organizations[58].

CHAPTER 3

EXPERIMENT

3.1 Basis of the Experiment

The cytotoxicity testing method employed in this work is the MTT assay. This testing method is modelled in several papers such as "Cytotoxicity of Carbon Nanomaterials: Single-Wall Nanotube, Multi-Wall Nanotube, and Fullerene" by Guang Jia et al. (2005) [53] and "Cytotoxicity of Graphene Oxide and Graphene in Human Erythrocytes and Skin Fibroblasts" by Ken-Hsuan Liao (2011) [14] et al. The reasons for using MTT assay over other techniques are the following:

- Proven technology: The utility of the MTT method has been documented in the literature for many different applications.
- Accurate measurements: The spectrophotometric procedure can detect slight changes in cell metabolism, making it much more sensitive than many other testing methods.
- Safer reagents: The reagents are safe to use and there's no need to store or manipulate harmful or radioactive substances, like in some of the other cases.
- Easy to use: The procedure is relatively simple and uses equipment already available in most labs.
- Rapid processing: Assays are run in a 96-well plate and read with a microtitre plate reader. These readers read the full plate at a time and thus allowing high-throughput handling of samples.
- Convenient storage: There is no problem of storage. The reagents are stable for 18 months when stored under refrigeration and in the dark.
- Reproducible results: The results obtained are reliable and reproducible, every time it is used. Also, the standards for testing using this method, are already established.

3.2 Materials Required

This testing method requires the following basic materials –

- Laminar flow hood – This was required to conduct experiments in a sterile contamination free environment.
- 37°C incubator - It is a conditioned environment for cell culture and cell storage.
- Microtiter plate reader – Elisa absorbance micro plate reader was used. The ability of the reader to reliably measure optical density (OD) is the key to this process.
- Inverted microscope – It was used for conducting cell counts.
- Reagents- MTT Reagent, Trypsin, PBS (phosphate buffer saline), DMEM (Dulbecco's Modified Eagle Medium), Sodium Dodecyl Sulfate (SDS) and Blue dye.
- Readily available cell culture - 3T3 and L929 cancer cells were used for cytotoxicity testing. The reason for using these cells is their ability to keep dividing. 3T3 cells that were used were mouse fibroblast cells and the L929 cells were human fibroblast cells. The images of 3T3 and L929 cells are shown in Fig 3.1 (a and b).

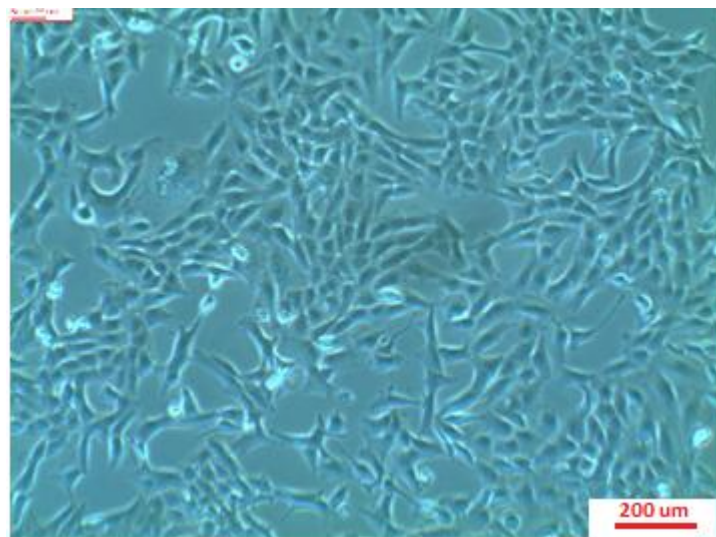


Figure 3.1: (a) Microscopic image of cultured 3T3 cells.

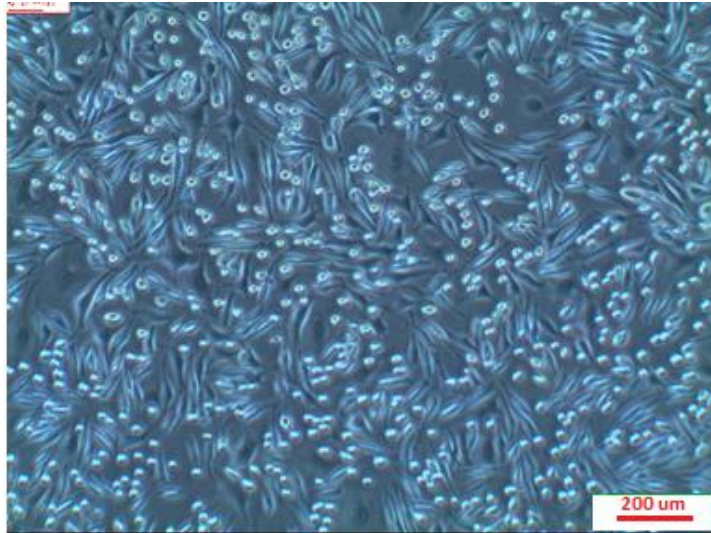


Figure 3.1: (b) Microscopic image of cultured L929 cells.

- Test material - The cytotoxicity assay was conducted for 5 types of nano materials – Carbon nanowire (100 ply), Graphene powder, Carbon nanotubes (multiwall carbon nanotubes, 10-20nm diameter, 1-2 μ m length, >99% pure, mfg. by SUNANO), Fullerene (99.5%) and Nanoclay (Cloisite 30B). The amount of material used per assay, was according to the standard specifications for cytotoxicity testing. According to the standard, the contact surface per ml of DMEM has to be 6cm²/ml or 3cm²/ml depending on the thickness of the material and for powder materials it has to be 10mg/ml of DMEM.
- Centrifuge – This was required for separation of material from DMEM.
- Vortex Mixer- This was required for mixing the material with DMEM.
- Other handling equipments - Sterile Microtiter plates (12x8=96 well plate), Multi-channel pipette, Sterile tubes (2ml), Serological pipettes and Sterile pipette tips (200 μ l, 100 μ l, 50 μ l).

3.3 Experimental Procedure

Sanitizing

The amount of nanomaterial required for test procedure was measured/weighed according to the standards (as mentioned section 3.2) and wrapped in aluminium foil. These were then autoclaved for 20min at 121°C.

TABLE 1

AMOUNT OF NANOMATERIAL AND DMEM USED FOR TESTING

MATERIAL	DIAMETER (mm)	LENGTH (mm)	AREA (mm²)	WEIGHT (mg)	DMEM ADDED (ml)
100 ply	1	110	346.97	17.8	1.13
Graphene	-	-	-	14.6	1.46
Nanoclay	-	-	-	6.6	0.66
Fullerene	-	-	-	18.6	1.86
Carbon Nanotubes	-	-	-	12.5	1.25

Medium separation and storage

After autoclaving, the materials were removed and stored in sterile 2 ml tubes along with the calculated amount of DMEM. The material was mixed thoroughly into DMEM (medium) using the Vortex mixer and stored at 37°C in the incubator. After every 2 days, starting from Day 1, the tubes were centrifuged, so as to separate the aggregated material from the medium. The rpm and the time for the centrifugation process were set in such a way so that only the large particles which failed to disperse into the solution separated. The fine particles which separated from the aggregated mixture and dispersed completely into the solution still remained in it. This was done because some materials like graphene, carbon nanotubes and nanoclay, imparted black/white colour to the medium. Since, the MTT test is a colorimetric test, this was not acceptable. The large aggregated particles were removed from the medium and only smaller particles which have completely dispersed into the medium

were allowed to remain. This was done for all powder based (graphene, nanoclay, carbon nanotubes and fullerene). So basically the testing materials were these fine nanomaterials evenly dispersed in the medium. After removal of the nanomaterial- rich medium, fresh medium was added to the tube with the material in it and again stored in the incubator. The process was continued every 2 days and hence test mediums were collected on Day 1, Day 3, Day 5, Day 7 and Day 10.

Stock Preparation from Cell Culture

In the meanwhile, 3T3 and 929 cells were cultured and grown in separate flasks. These cells are attached to the bottom of the container and immersed in a layer of medium which facilitates growth. The medium was poured out and the flask was rinsed using PBS. The rinsing was mild so as to not detach the cells from the bottom of the flask. Around 5 ml of Trypsin was then added to it. Trypsin is an enzyme of pancreatic juice that hydrolyzes proteins and converts them into smaller polypeptide units. When added, Trypsin removes the cells stuck to the bottom of the flask. After 3 minutes, about 6ml of medium was added to the cell solution so as to stop the activity of Trypsin. This is done to prevent the cells from getting eaten away by Trypsin. The solution was thoroughly mixed so as to make sure that all the cells from the bottom have detached and separated and not agglomerated. This cell solution is called stock.

Cell Count

20 μ l of stock was taken and 20 μ l of blue dye was added to it. After mixing it was put on a Neubauer slide (fig 3.2). To prepare the counting chamber the mirror-like polished surface of the slide was cleaned. A clean cover slip was taken and placed over the counting surface before the dyed stock was introduced. Cover slips for counting chambers are thicker than those for conventional microscopy because they must be heavy enough to overcome the surface tension of a drop of liquid. The dyed stock was then introduced into one of the V-

shaped wells with a pipette tip. The area under the cover slip fills up by capillary action. Enough stock should be introduced so that the mirrored surface is completely covered. The counting chamber was then placed on the microscope stage and brought into focus at low power.

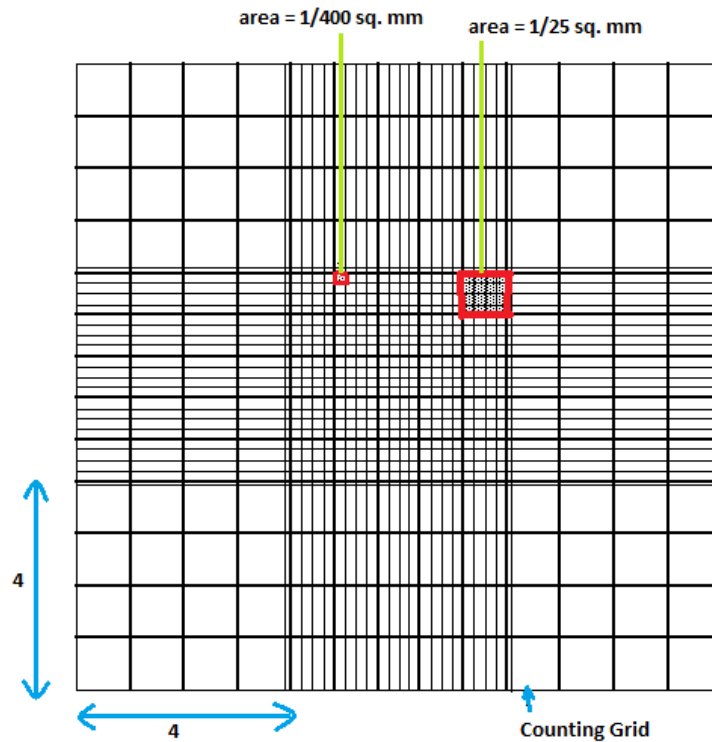


Figure 3.2: Representation of Neubauer slide

Calculations

The cells in each counting grid were counted and an average was taken. The volume of each counting grid is 0.1 μ l.

$$\begin{aligned} \text{Average cell count} &= 112 \text{ cells} / 0.1 \mu\text{l} \\ &= 112 \times 10^4 \text{ cells} / \text{ml} \end{aligned}$$

After including the dilution factor (blue dye that was added to the stock) it comes out to:

$$= 112 \times 10^4 \times 2 \text{ cells} / \text{ml}$$

To calculate the amount of stock that should be added to the 96 well plate, the Mass balance Equation was used:

$$C_1 V_1 = C_2 V_2$$

Where,

C_1 = the concentration of the stock solution. = $112 \times 10^4 \times 2$ cells /ml

V_1 = the volume of stock solution used (unknown)

C_2 = final concentration of diluted stock solution = 10^5 cells/ml (standard)

V_2 = final volume of diluted stock solution = $100 \mu\text{l/well}$ (standard) = 10ml/plate

(Assuming it is a 100 well plate)

During the several tries that were performed, different nanomaterials were tested at different times. So, to make the details of the calculation more general, let us suppose that at a time "S" number of materials were tested. Accordingly we will have to multiply V_2 by the factor "S".

Substituting the values in the above equation, we get V_1 . During a particular trial, 4 materials were tested. Therefore, S was taken as 4.

$$V_1 = (10^5 \times 4 \times 10) / (112 \times 10^4 \times 2) = 1.78 \text{ ml}$$

1.78 ml of stock was taken and added to 38.22ml of medium so as to get a total of 40 ml of final diluted stock. $100 \mu\text{l}$ of this stock was taken and added to each well of the 96 plate. The plates were then put in the incubator for 1 day to allow the cells from the stock to get attached to the bottom of the plate. One plate was used for each material.

Addition of the refrigerated material medium

The test mediums that were refrigerated were diluted to varying degrees by adding new fresh medium to it and then added to the 96 well plate. The dilution was done in the following way:

$100 \mu\text{l}$ of material medium was mixed into 100 ml of fresh medium = 1:1

$100 \mu\text{l}$ of material medium was mixed into $200 \mu\text{l}$ of fresh medium = 1:2

$100 \mu\text{l}$ of that 1:2 solution was mixed with $100 \mu\text{l}$ of fresh medium = 1:4

100µl of that 1:4 solution was mixed with 100µl of fresh medium = 1:8

100µl of that 1:8 solution was mixed with 100µl of fresh medium = 1:16

100µl of that 1:16 solution was mixed with 100µl of fresh medium = 1:32

100µl of that 1:32 solution was mixed with 100µl of fresh medium = 1:64

100µl of that 1:64 solution was mixed with 100µl of fresh medium = 1:128

These diluted solutions were then added to the 96 well plate. SDS and fresh medium was also added to the cell culture (rows 9-12) which act as references points. Medium has no effect on cell growth and is not cytotoxic where as SDS kills all the cells. By adding them to the cell culture we created 2 reference points between which, all the others should lie. The SDS solution was made in the following way:

8µl of 10% SDS was mixed into 1 ml of PBS = 0.8mg/ml

500µl of 0.8mg/ml was mixed with 500µl of PBS = 0.4mg/ml

500µl of 0.4mg/ml was mixed with 500µl of PBS = 0.2mg/ml

50µl of SDS was mixed into 100µl of medium and 150µl of medium = 0.1mg/ml and 0.05mg/ml resp.

TABLE 2

SAMPLE SOLUTION, SDS AND THE MEDIUM IN A 96 WELL PLATE.

		1	2	3	4	5	6	7	8	9	10	11	12
Day 0-1	A	1:1	1:2	1:4	1:8	1:16	1:32	1:64	1:128	SDS1:1	SDS1:1	Medium	Medium
Duplicate	B	1:1	1:2	1:4	1:8	1:16	1:32	1:64	1:128	SDS1:2	SDS1:2	Medium	Medium
Day1-3	C	1:1	1:2	1:4	1:8	1:16	1:32	1:64	1:128	SDS1:4	SDS1:4	Medium	Medium
Duplicate	D	1:1	1:2	1:4	1:8	1:16	1:32	1:64	1:128	SDS1:8	SDS1:8	Medium	Medium
Day 3-5	E	1:1	1:2	1:4	1:8	1:16	1:32	1:64	1:128	SDS1:16	SDS1:16	Medium	Medium
Duplicate	F	1:1	1:2	1:4	1:8	1:16	1:32	1:64	1:128	SDS1:32	SDS1:32	Medium	Medium
Day 5-7	G	1:1	1:2	1:4	1:8	1:16	1:32	1:64	1:128	SDS1:64	SDS1:64	Medium	Medium
Duplicate	H	1:1	1:2	1:4	1:8	1:16	1:32	1:64	1:128	SDS1:128	SDS1:128	Medium	Medium

Duplicates of were also prepared and added to the adjacent wells. This was done to get more reliable results. The plates were then kept in the incubator for 3 days.

Addition of MTT

On the third day 20 μ l of MTT was added to each well and kept in the incubator for 6 hours. MTT is a yellow tetrazolium salt [3-(4, 5-Dimethylthiazol-2-yl)-2, 5-diphenyltetrazolium-bromide] which is metabolized by mitochondrial succinic dehydrogenase activity of proliferating cells to yield a purple formazan reaction product. After 6 hours, the solution in the well plates turn to various shades of blue/purple. They were then emptied and 200 μ l of 10% SDS was added to each well to kill all the cells and retain the acquired blue/purple colour.

Plate Reading

The next day the plates were read by measuring the optical density (absorbance) using a spectrophotometer. It is a logarithmic ratio of the radiation falling upon a material, to the radiation transmitted through a material. The wavelength used was 590 nm. Deeper the blue colour, higher is the absorbance and higher is the value of absorbance. Lighter the colour, higher is the transmittance and lower is the value of absorbance. These absorbance values were taken and noted and graphs were plotted to get a relative measure of values.

General note

Several tries were carried out and each try involved a different set of samples. The calculations mentioned in the previous section refer to the values of only one of those tries. The calculation depends on initial number of cells in the culture, the volume of the medium, the number of samples etc. Viability graphs (in %) were plotted from the readings obtained from the spectrophotometer, which take these initial differences into consideration and bring the results from all the experiments on same scale (out of 100).

Before performing the above mentioned experiment, preliminary tests were also carried out, especially with carbon nanowire. These tests were performed with the actually material in the cell culture and not the medium. The main reason why this was done was because the carbon nanowire, unlike the other nanomaterials, is not in a powder form. Thus, it was necessary to make sure that the results with the actual material in the cell culture were similar to the results with only the nanomaterial-rich medium in the cell culture. This was also done so as to get a general idea on how the main experiment should be carried out. However the results from the preliminary tests have also been reported in the next chapter because it gives an important analysis for the main experiment.

CHAPTER 4

RESULTS AND ANALYSIS

4.1 Preliminary Results

As mentioned in the previous chapter, the preliminary test on carbon nanowire was performed to see the effect of introducing the nanomaterial as a whole into the cell culture. Emphasis was laid only on carbon nanowire because the other nanomaterials were powdered and it was not possible to do an MTT test by introducing them directly since they imparted their own colour to the cell culture. The preliminary test was compared to the main test in which only the medium in which the nanomaterial was soaked was used. After performing the MTT assay, the spectrophotometer readings were obtained at OD 590 (optical density, 590nm), which are as given below:

TABLE 3
OD READINGS FROM THE PRELIMINARY TESTS OF PRISTINE 100 PLY CARBON NANOWIRE

	1:1	1:2	1:4	1:8	1:16
Day 0	1.00	1.00	1.13	1.02	0.95
Day 1	0.99	1.01	1.13	1.09	1.17
Day 2	0.86	0.94	1.02	0.98	1.05
SDS	0.04	0.06	0.04	0.04	0.05
Medium	1.04	1.08	1.13	1.21	1.37

These readings in Table 4.1 were taken at OD 590, up to a dilution of 1:16 till day 5. Viability, here, is defined as the ability of the cells (in a cell culture) to grow and reproduce in the presence of a nanomaterial. Based on the OD readings, the viability can be calculated in the following way.

$$\text{Viability} = (\text{OD reading of sample} / \text{Average OD reading of Medium}) \times 100$$

Viability is a more informative scale as compared to the OD reading scale because for different trials, the OD readings for the samples might differ. Viability takes that difference into consideration and gives the value in percentages.

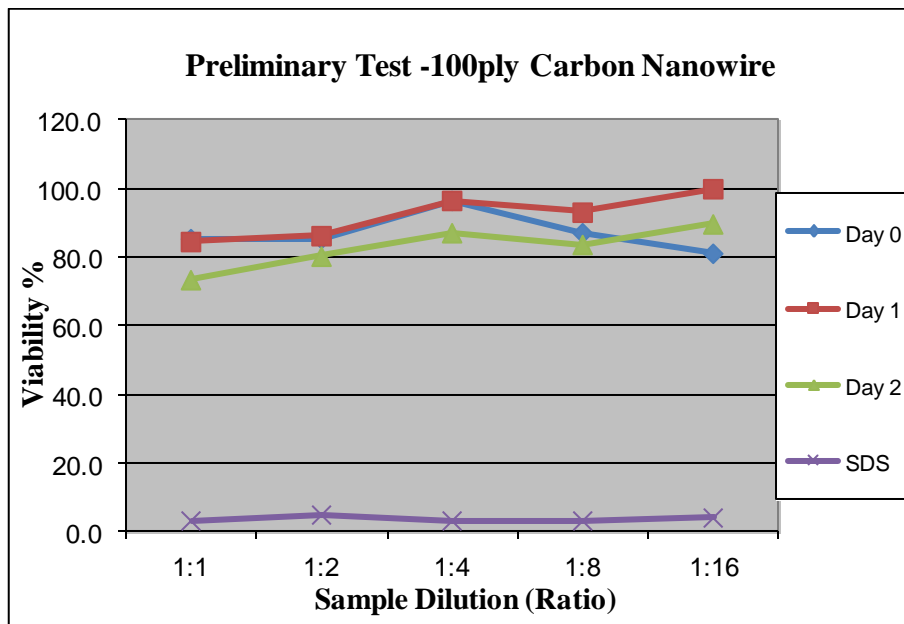


Figure 4.1: Graph showing Viability vs Sample Dilution for pristine 100ply Carbon Nanowire on 3T3.

The graph in figure 4.1 shows the viability values of 100 ply pristine Carbon nanowires. For a material to be considered safe, viability over 70% is considered acceptable because beyond this there is little or no apoptosis [45]. From the graph, we can see that the viability values for days 0-2 range from 84% – 100%, well beyond the safe range, which is contrary to the established notion about nanomaterials being cytotoxic. Also, from the graph, the viability is constant with increase in dilution, the reason for which has been discussed in the main results. During the preliminary tests, cell contamination was common, wherein the viability would show a sudden depression. The problem of contamination was taken care of by carrying out the main experiments in an extremely clean environment under a fume hood. This experiment gave an insight into how the main experiment should be carried plus it gave encouraging toxicity results for carbon nanowire.

4.2 Main Results

Cytotoxicity of pristine 100ply carbon nanowire, graphene and carbon nanotubes were tested on 3T3 and L929 cancerous cells. 3T3 cells were obtained from mouse fibroblast and L929 were obtained from human fibroblast. The reason for choosing two cell types was to check if the effect of cytotoxicity was cell dependent. Prior to the assay SEM and TEM images (fig 4.2 (a, b and c)) were taken of carbon nanowire, graphene and carbon nanotubes, so as to get a closer look at their structures.

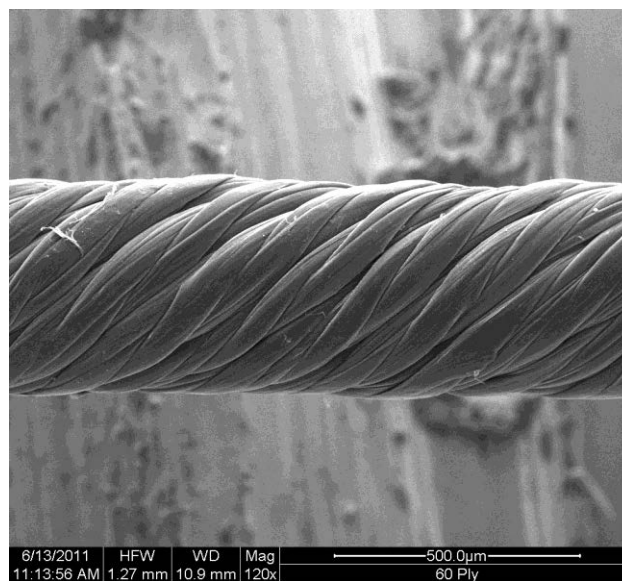


Figure 4.2 (a): SEM image of 100 ply pristine carbon nanowire.

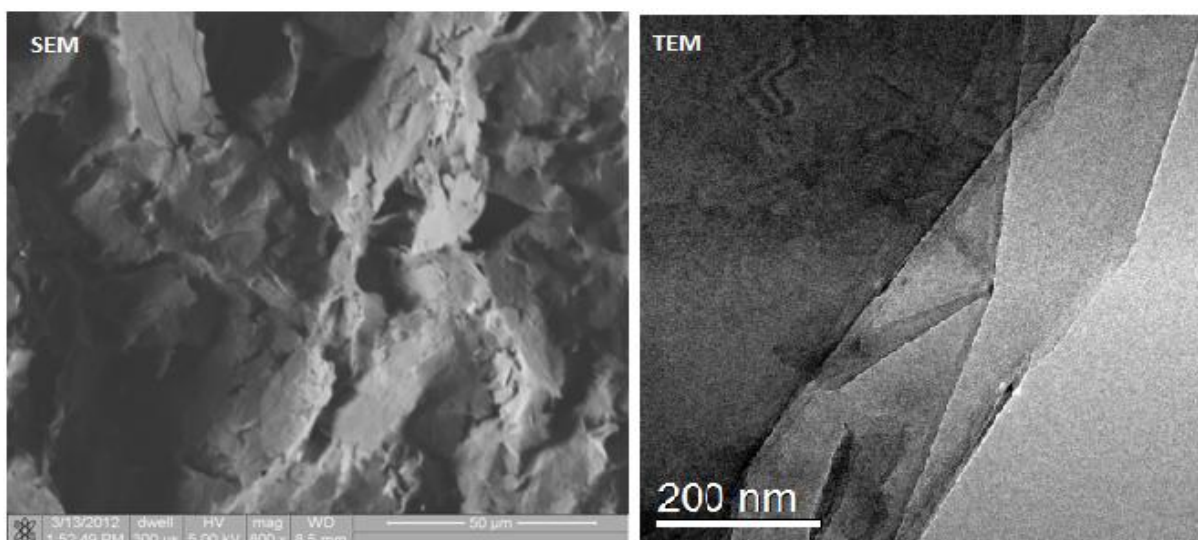


Figure 4.2 (b): SEM and TEM images of graphene powder/flakes.

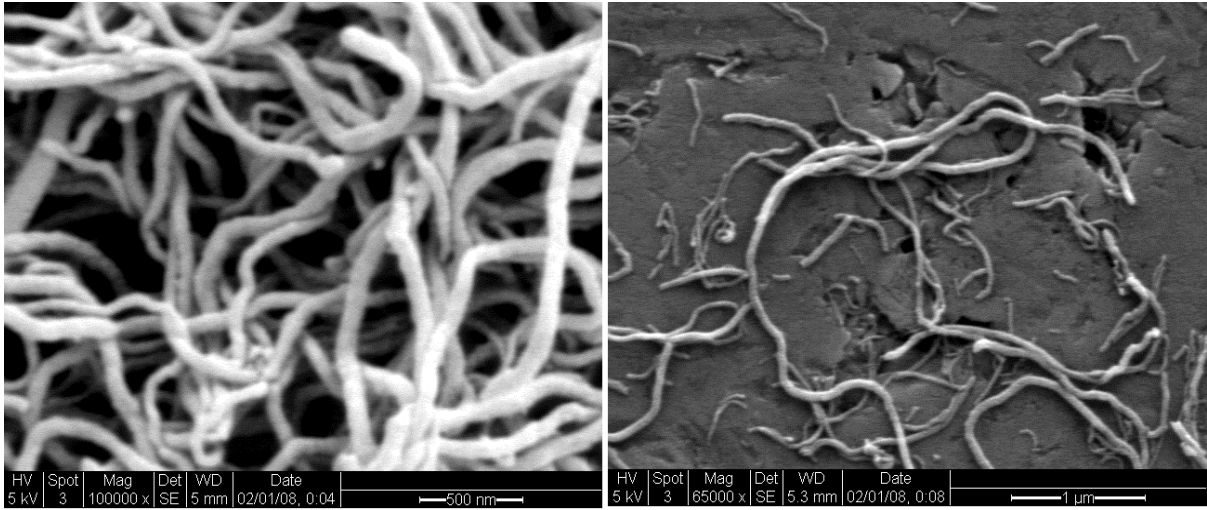


Figure 4.2 (c): SEM image of Multiwall Carbon Nanotubes.

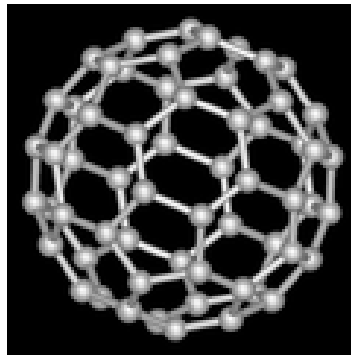


Figure 4.2 (d): 3-D model of C60 Fullerene [16].

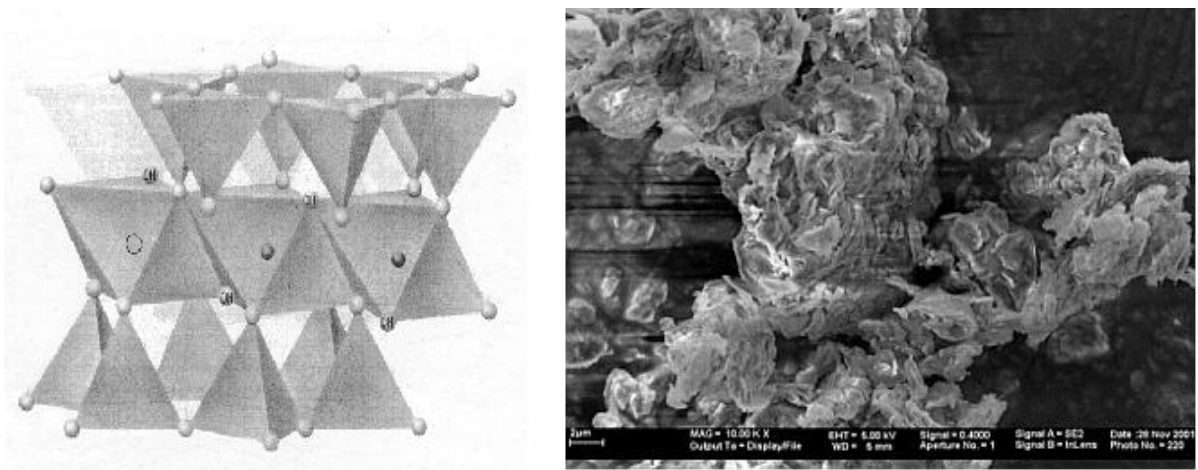


Fig 4.2 (e): SEM image of Nanoclay [61]

TABLE 4

OD 590 READINGS FOR CARBON NANOWIRE, GRAPHENE, AND CARBON NANOTUBE.

OD 590	3T3	1:1	1:2	1:4	1:8	1:16	1:32	1:64	1:128
Carbon Nanowire	Day 3	2.63	2.94	2.84	2.80	2.94	2.86	2.85	2.84
	Day 5	2.64	2.71	2.61	2.59	2.81	2.67	2.56	2.73
	Day 7	2.51	2.38	2.41	2.31	2.46	2.39	2.35	2.60
	Day 10	2.53	2.45	2.54	2.41	2.52	2.38	2.49	2.46
	SDS	0.04	0.04	0.04	0.04	1.15	2.30	1.95	2.57
	Medium	2.93	2.98	2.79	2.80	2.99	3.09	2.26	2.91
Graphene	Day 3	0.04	0.04	1.04	1.59	1.93	2.26	2.37	2.42
	Day 5	0.13	1.33	1.75	2.15	2.23	2.54	2.94	3.01
	Day 7	0.85	1.54	1.84	2.15	2.41	2.71	2.89	2.81
	Day 10	1.00	1.52	1.79	2.03	2.25	2.17	2.62	2.48
	SDS	0.04	0.04	0.04	0.04	0.53	2.29	2.35	2.28
	Medium	2.66	3.05	3.03	3.18	3.23	3.26	3.23	2.63
Carbon nanotube	Day 3	1.29	1.44	1.68	1.88	1.96	2.21	2.26	2.57
	Day 5	1.13	1.70	1.86	2.26	2.11	2.87	2.83	3.09
	Day 7	1.17	1.39	1.88	2.11	1.70	2.58	2.71	3.06
	Day 10	1.27	1.50	1.43	1.69	2.21	2.29	2.38	2.53
	SDS	0.04	0.04	0.04	0.04	1.05	2.73	2.41	2.23
	Medium	2.60	3.37	2.97	2.61	2.86	2.92	3.02	2.46

From the figure 4.2(a), 100 threaded structure of the carbon nanowire can be seen. In the picture 100 such threads of carbon nanotubes are twisted together to form a tight single consolidated wire. In figure 4.2(b) the surface of the graphene flake can be seen. It is uneven and the texture is very soft and powdery. The particle distribution of the graphene powder that was used in the experiment was large. In figure 4.2(c) the tube-like structure of carbon

nanotubes are shown, they can be seen crisscrossing and are haphazardly arranged. The particle distribution of the carbon nanowire used was very small. All the particles had diameter ranging from 10-20nm and length 1-2 μm . In figure 4.2(d) the truncated icosahedron structure of the C60 makes it a close packed structure. There are no open bonds present, which might participate in reactions and is stable. Figure 4.2(e) shows plate like structure where the individual plate thickness is just about 1 nm but surface dimensions are 300-600 nm. Its external appearance is fine and is powdery. The density of nanoclay was much more; or the same volume of powder, nanoclay weighed almost twice as much as graphene.

The table 4.2 gives the OD590 values for cytotoxicity testing of 100ply Carbon nanowire, Graphene and Carbon nanotubes on 3T3 cells.

4.2.1 OD590 - Carbon Nanowire - 3T3

For 100 ply carbon nanowire, the OD values are more or less the same and there does not seem to be any change in the values with increase in dilution. This might mean that the cells are independent of the concentration of the carbon nanowire. As we go down along a column, there is no significant change, only a very slight decrease. The time duration has very little effect on the cytotoxicity of carbon nanowires. The slight decrease might be due to weakening of the threaded structure of the nanowire. As the threads weaken, some nanotubes are introduced into the medium and this brings down the OD reading.

4.2.2 OD590 - Graphene - 3T3

Graphene on the other hand shows extremely low OD values which increase drastically with increase in dilution. This means that the cytotoxicity level of graphene at higher amounts, is very high and at lower (1:128) concentrations it is almost nil. Usually the percentage of single layer present in a graphene powder is 80. Due to this the contact with the medium is very intimate. At 1:1 concentration, with increase in time duration, the

cytotoxicity of graphene decreases. This means that it is toxic in the initial few days and with time, its effect reduces. The main reason why this kind of behaviour is seen is because of the large particle distribution of graphene. The method of separation of graphene from the medium (as was mentioned earlier) was by centrifugation. During this process only the large aggregated particles are separated. The smallest of the lot remain dispersed in the solution. The particles smallest ones remain in the medium, separated on the 1st day and the larger ones separated on the last day.

4.2.3 OD590 - Carbon Nanotubes - 3T3

Carbon nanotubes show intermediate OD values, which means that their cytotoxicity levels are lower than carbon nanowire and higher than graphene. As compared to graphene the carbon nanotubes have tube like structures which means the surface interaction with the medium is lesser. The OD values increase on increasing the dilution. The cytotoxicity level is low at lower concentrations. The effect of time duration on cytotoxicity is mixed. There is slight increase in cytotoxicity at some dilutions while slight decrease in others. After conversion of the OD values to viability values, graphs as given in were constructed.

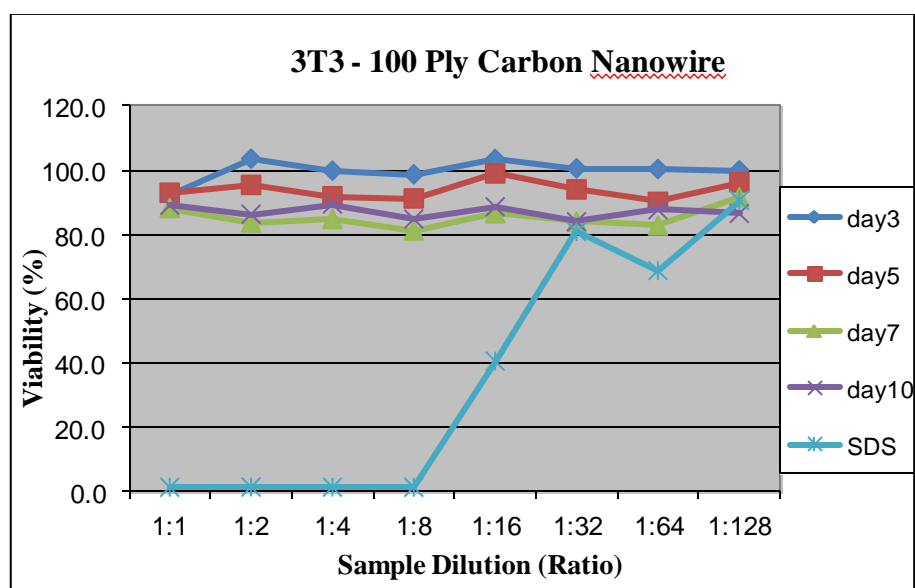


Figure 4.3: Graph showing the Viability vs Sample Dilution results of carbon nanowire on 3T3 cells.

4.2.4 Viability Graph - Carbon Nanowire - 3T3

In case of carbon nanowire (fig 4.2), the dilution has no effect in the viability. This is because the nanotubes are threaded together and are not free to move around. The surface area in contact with the medium remains the same no matter how much medium is added to it. Due to this the viability is constant at a given time. With the increase in time duration, the viability decreases. As discussed previously, with increase in soaking time, the threaded bonds might weaken and release some nanotubes into the solution. But, the overall viability of the nanowire is about 87% which makes it compatible to live 3T3 cells.

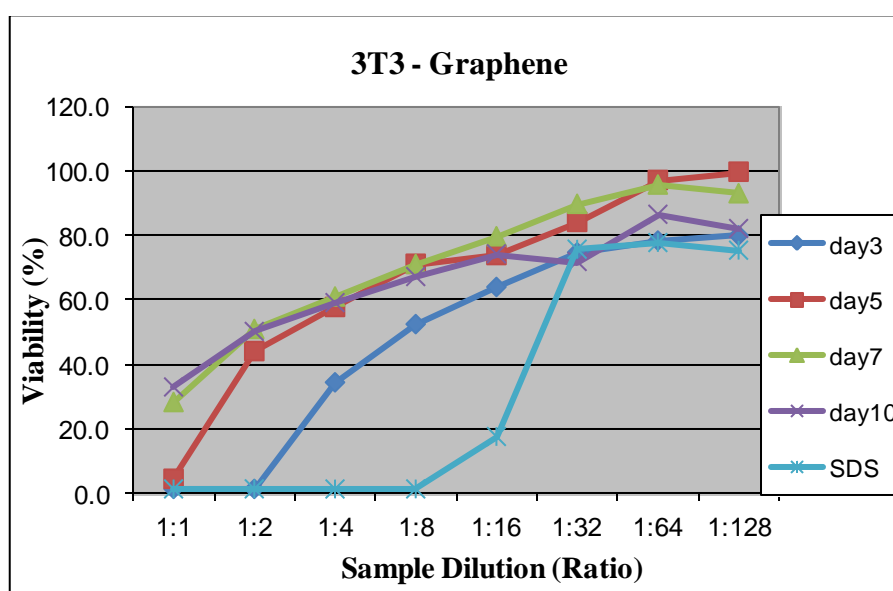


Figure 4.4: Graph showing the Viability vs Sample Dilution of graphene on 3T3 cells.

4.2.5 Viability Graph - Graphene - 3T3

Graphene (fig. 4.3) on the other hand, shows a completely different behaviour as compared to carbon nanowire. Unlike carbon nanowire, dilution has a marked effect on the viability of graphene. With increase in dilution, the viability of graphene increases, which means that at lower concentrations the number of cell deaths is very low. The viability is within the safe range (<80%) only beyond a dilution of 1:16, which means that the concentration of graphene has to be below 0.58mg/ml to be considered safe. The effect of time durations is inverse to what was seen in case of carbon nanowire. Here, with increase in

time duration, the viability increases. It increases from 0% to almost 30%. The reason for this behaviour has been discussed further.

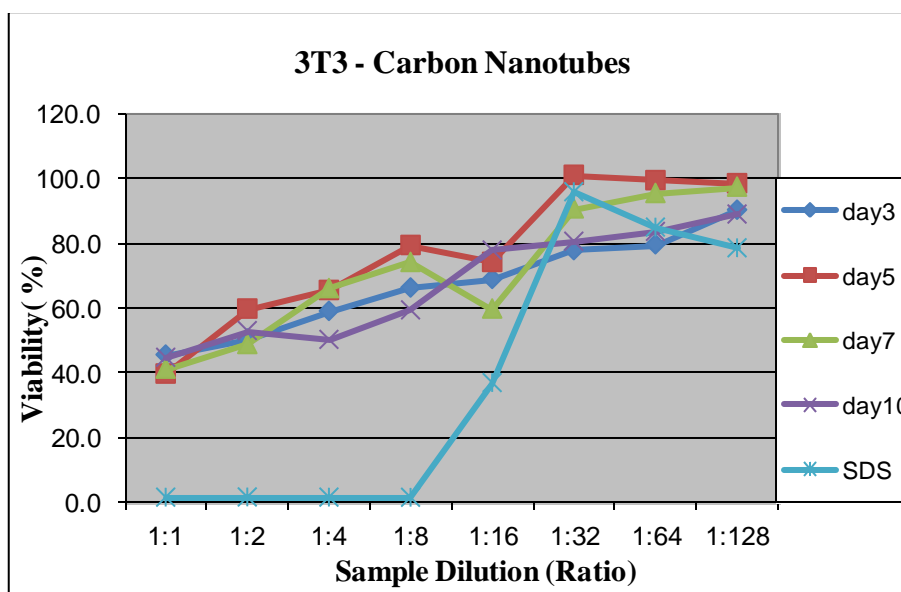


Figure 4.5: Graph showing Viability vs Sample Dilution of Carbon Nanotubes on 3T3 cells

4.2.6 Viability Graph - Carbon Nanotubes - 3T3

Carbon nanotubes (fig. 4.4) show viability between carbon nanowire and graphene. With increase in dilution the viability increases. At concentrations below 1:16, Carbon nanotube has viability over 80%, which makes it biocompatible with 3T3 cells below a concentration of about 0.58 mg/ml. The time duration, as discussed previously, shows a mixed trend. The graph lines are overlapping and crisscrossing. The time duration does not seem to have any significant effect of carbon nanotubes on 3T3 cells. Between carbon nanotubes and graphene, the reason why graphene shows higher cytotoxicity is because of its needle-like structure (due to high aspect ratio) which can cut through cells and eventually kill them, whereas carbon nanotubes have a tube-like structure and do not slice through cells. Tests conducted on L929 human fibroblast cells have been discussed further and compared with the results obtained from cytotoxicity studies on 3T3 mouse fibroblast cells.

As was discussed in the experiment section, SDS and medium were added to the cells to get two reference points for toxicity testing. Cells are compatible with medium where as they are incompatible with SDS. As the amount of SDS increases the percentage of cell death increases. Images of these cells in the above given reagents were taken and are shown in figure 4.6 and 4.7 (a-d).

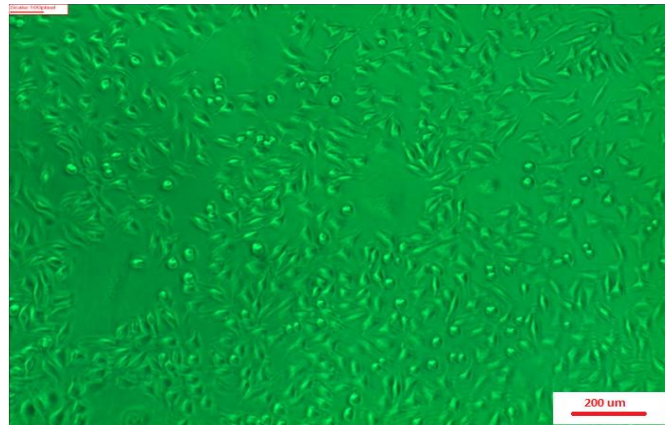


Figure 4.6: Image of L929 cells in medium (DMEM)

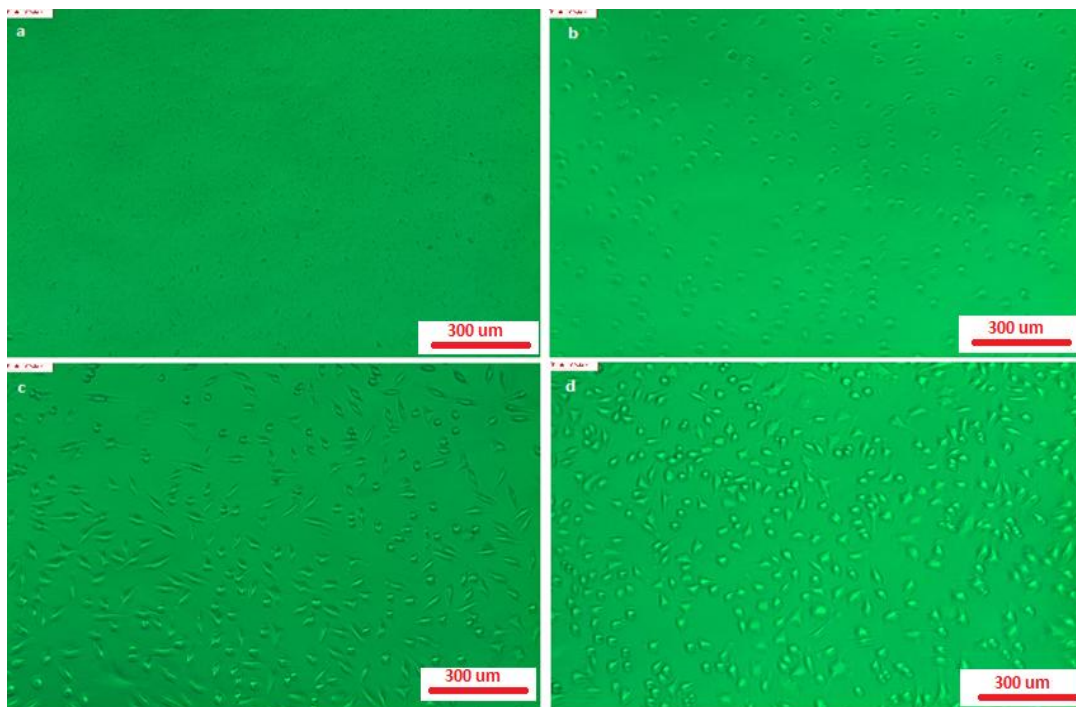


Figure 4.7: (a) Image of 929 cells in SDS in 50% SDS (1:1 ratio). (b) Image of 929 cells in SDS in 33.3% SDS (1:2 ratio).(c) Image of 929 cells in SDS in 20% SDS (1:4 ratio). (d) Image of 929 cells in SDS in 11.1% SDS (1:8 ratio).

The table 4.3 shows the OD590 readings of pristine 100 ply carbon nanowire, graphene and carbon nanotubes from a dilution of 1:1 to 1:128, through days 3-10 on L929 cells.

TABLE 5

OD 590 READINGS OF PRISTINE 100PLY CARBON NANOWIRE, GRAPHENE, AND CARBON NANOTUBES ON L929 CELLS.

OD 590	L929	1:1	1:2	1:4	1:8	1:16	1:32	1:64	1:128
100 ply	Day 3	0.69	0.75	0.78	0.78	0.75	0.89	0.80	0.81
	Day 5	0.58	0.52	0.56	0.65	0.69	0.73	0.75	0.68
	Day 7	0.51	0.51	0.56	0.60	0.60	0.60	0.67	0.66
	Day 10	0.49	0.53	0.55	0.61	0.60	0.62	0.70	0.64
	SDS	0.04	0.04	0.04	0.04	0.90	0.90	0.86	0.87
	Medium	0.93	0.94	0.84	0.74	0.72	0.68	0.73	0.70
Graphene	Day 3	0.04	0.04	0.74	0.83	0.97	1.02	0.85	0.86
	Day 5	0.40	0.58	0.74	0.87	0.88	0.92	0.82	0.80
	Day 7	0.48	0.61	0.65	0.69	0.68	0.69	0.86	0.75
	Day 10	0.53	0.67	0.74	0.78	0.78	0.76	0.85	0.84
	SDS	0.04	0.04	0.04	0.04	0.58	0.58	1.04	1.09
	Medium	1.04	1.04	0.95	0.98	0.94	0.89	0.95	1.06
Carbon Nanotube	Day 3	0.50	0.60	0.62	0.70	0.81	0.79	0.87	0.90
	Day 5	0.50	0.61	0.66	0.76	0.81	0.91	1.04	1.11
	Day 7	0.51	0.53	0.77	0.66	0.70	0.71	0.80	0.66
	Day 10	0.54	0.59	0.59	0.60	0.65	0.72	0.74	0.80
	SDS	0.04	0.04	0.04	0.04	0.04	1.28	1.04	1.13
	Medium	1.11	1.07	0.96	1.00	0.95	1.00	0.93	1.12

4.2.7 OD590 - Carbon Nanowire - L929

In case of carbon nanowire, the OD readings, very slightly increase but on the whole, remain more or less constant, with increase in dilution. With increase in time duration, the

OD readings decrease, which means that the cytotoxicity levels go up. The average OD readings on day 3 are higher than that on day 10. This trend can be attributed to the same reason as was discussed previously, that, with increase in soaking time the carbon nanowire becomes weaker and the carbon nanotubes start dispersing in the medium. The behaviour is similar to 3T3 cells but not identical.

4.2.8 OD590 - Graphene - L929

At high concentrations the OD readings for graphene is very low, i.e it is highly toxic. The OD readings for graphene increase with increase in dilution. Graphene is compatible with L929 cells only below a concentration of 0.58mg/ml. The standard concentration which was used for this cytotoxicity testing is too high for Graphene. It is safe to use only beyond a dilution of 1:16. The effect of time duration at 1:1 concentration is same as what was seen earlier on 3T3 cells. With increase in time duration the viability increases. The reason why this can be seen is because the medium separated on day 1 has the smallest particles. Smaller particles are more capable of cutting through the cells and killing them as compared to larger particles. This finding is according to those of Liao et.al [14], where in the smallest size, graphene oxide showed the greatest hemolytic activity, whereas aggregated graphene sheets exhibited the lowest hemolytic activity. Here with the increase in time the OD readings decrease. There seems to be an effect of the cell type on the trend of cytotoxicity with time duration.

4.2.9 OD590 - Carbon Nanotubes - L929

In case of Carbon Nanotubes, with increase in dilution the OD readings increase gradually. The increase from one dilution to the next is almost equal. The cytotoxicity is less at lower concentrations and increases with increase in dilution. The time duration again shows a mixed trend, as was seen earlier in 3T3 cells. Between carbon nanotubes and graphene, carbon nanotubes are more hydrophobic as studied by Bottini et.al [48] in his paper

titled “Multiwalled Carbon Nanotubes Induce T-Lymphocyte Apoptosis” where he mentions that pristine carbon nanowires are hydrophobic and less toxic.

The viability graphs that were derived from the OD readings have been discussed further.

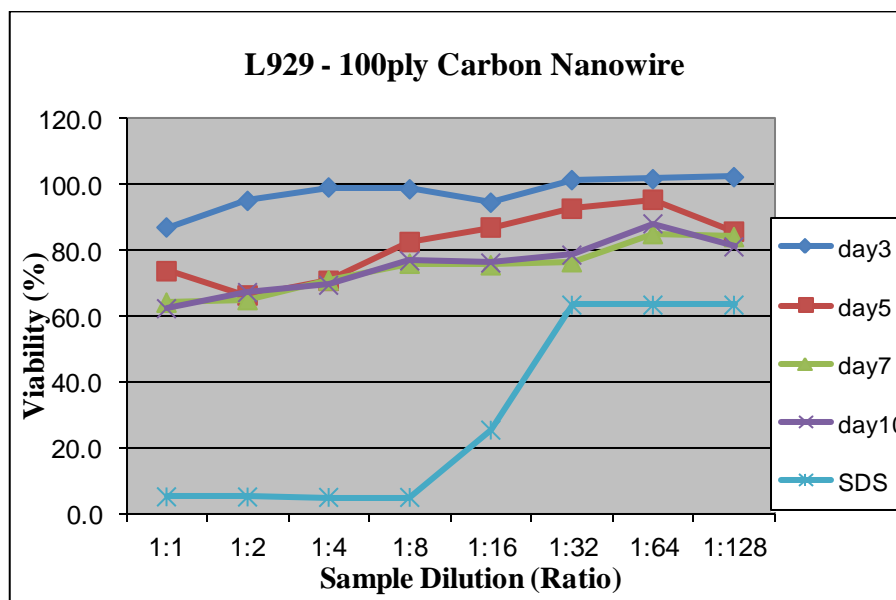


Figure 4.8: Graph showing the Viability vs Sample Dilution of 100Ply carbon nanowire on L929 cells.

4.2.10 Viability Graph - Carbon Nanowire - L929

In the graph in Figure 4.5, dilution has minimal effect on the viability of carbon nanowire. This feature can be attributed to the same reason that was discussed earlier in section 4.2.1 and 4.2.4. As compared to the graph obtained in section 4.2.4 for 3T3 cells, the graph in this case is more spread out. That is, the range between the maximum and the minimum viability values is more. The average however is almost the same. Again, with increase in time duration, there is a decrease in viability which also can be attributed to the same reason. As can be seen from the cell structures of 3T3 and L929 in figures 3.1 a and b, the surface area of contact is expected to be more in L929 than 3T3 cells. Due to larger surface area, the interaction with the cells is increased.

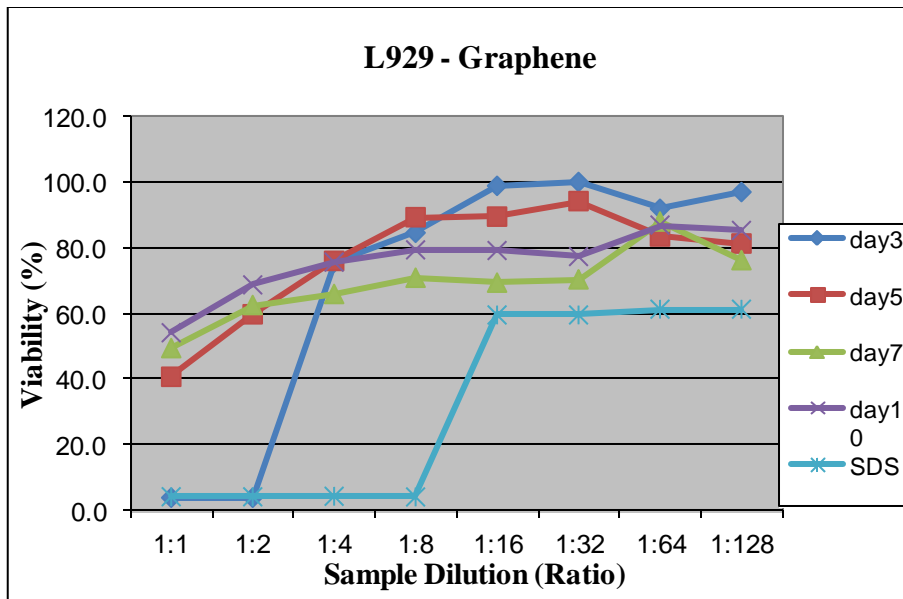


Figure 4.9: Graph showing the Viability vs Sample Dilution of graphene on L929 cells.

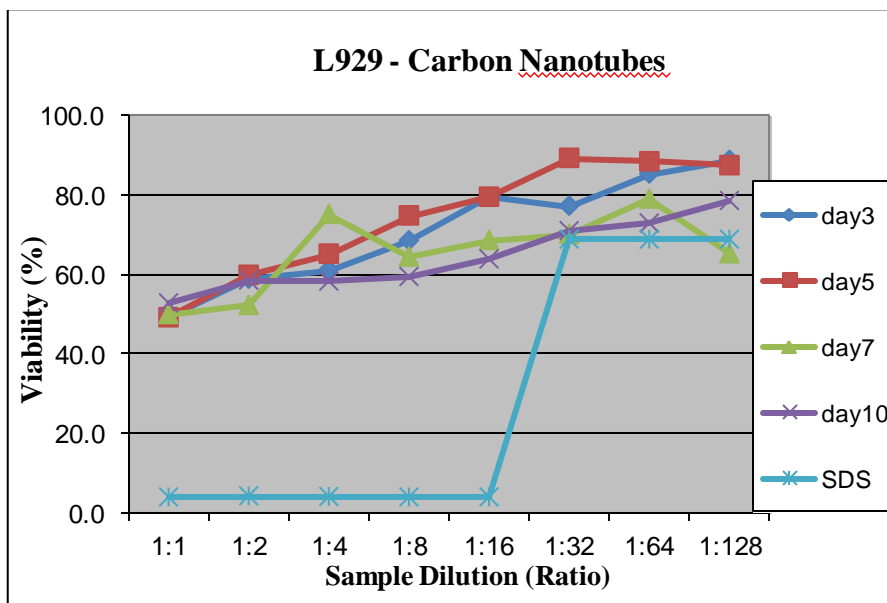


Figure 4.10: Graph showing the Viability vs Sample Dilution of carbon nanotubes on L929 cells.

4.2.11 Viability Graph - Graphene - L929

As can be seen in the graph in Figure 4.6, with increase in dilution, the viability increases. At 1:1 ratio the viability is about 45% and at around a dilution of 1:16, the viability increases to 80%. The trend is similar to what was seen in 3T3 cells, the only difference being; in 3T3 the increase was steep, since the viability was around 10% at 1:1 ratio for all

the days. Here the viability for days 3, 5, 7 and 10 it varies between 40% and 50%. The sequence in which the viability increases from day 1 to day 10 shows the same trend as was seen and discussed earlier.

4.2.12 Viability Graph- Carbon Nanotubes - L929

The viability in the graph in figure 4.7 increases with increase in dilution. At a dilution of about 1:16 the viability is 80%, which increases with further increase in dilution. The time duration again shows a mixed trend, as was seen in 3T3 cells. Comparing the graphs 4.5 and 4.10, it can be seen that the behaviour is almost identical. In all the cases, the viability of carbon nanotubes in contrast to graphene shows one single value at 1:1 concentration. The reason why the graphs of carbon nanotubes start at single point is because of the narrow range of particle size distribution. Almost all the particles have the same size and are dispersed in the medium in the same way. For a given particle size, the viability of a material remains almost the same.

From the above study, the shape of the graphs obtained for pristine 100ply Carbon Nanowire and Carbon Nanotubes and graphene were consistent, both in terms of dilution and the time duration.

Looking at the similarity in the graphs for both 3T3 and L929 cells, cytotoxicity tests of nanoclay and fullerene were conducted directly on human fibroblast cells (L929). Nanoclay and fullerene were chosen because of their potential to be used in a number of applications (Discussed in Literature Review, Chapter 2) and the little work done in cytotoxicity studies of these materials.

The OD readings of the cytotoxicity tests of Graphene, Nanoclay and Fullerene upto a dilution of 1:128 for days 1-7 are given in Table 4.4.

TABLE 6

OD 590 READINGS OF PRISTINE 100PLY GRAPHENE, CARBON NANOTUBES, FULLERENE AND NANOCCLAY ON L929 CELLS.

	L929	1:1	1:2	1:4	1:8	1:16	1:32	1:64	1:128
Graphene	Day 1	0.04	0.25	0.71	0.91	0.98	1.01	1.10	1.13
	Day 3	0.41	0.76	0.96	1.04	1.12	0.89	0.97	1.32
	Day 5	0.47	0.61	0.84	1.00	1.11	1.02	1.02	1.34
	Day 7	0.50	0.46	0.71	0.89	1.09	1.31	1.35	1.50
	SDS	0.05	0.04	0.04	0.04	0.49	0.49	1.06	1.56
	Medium	1.49	1.60	1.02	1.78	1.59	1.48	1.67	1.55
Nanoclay	Day 1	0.04	0.30	0.69	1.07	1.31	1.31	1.42	1.38
	Day 3	0.04	0.24	0.59	0.93	1.26	1.36	1.42	1.33
	Day 5	0.04	0.33	0.71	1.13	1.37	1.44	1.46	1.32
	Day 7	0.05	0.28	0.57	0.83	1.10	1.22	1.37	1.34
	SDS	0.04	0.04	0.04	0.04	0.65	0.65	1.06	1.56
	Medium	1.48	1.50	1.40	1.49	1.42	1.41	1.54	1.63
Fullerene	Day 1	0.98	1.02	1.22	1.29	1.40	1.44	1.48	1.39
	Day 3	1.61	1.51	1.25	1.50	1.66	1.45	1.26	1.37
	Day 5	1.30	0.80	1.01	1.09	1.12	1.35	1.64	1.51
	Day 7	0.99	0.88	0.97	1.13	1.10	1.31	1.32	1.16
	SDS	0.045	0.046	0.038	0.040	0.65	0.65	1.06	1.46
	Medium	1.682	1.726	1.521	1.694	1.530	1.594	1.597	1.834

In this experiment, the effect time duration on viability of graphene, did not show any fixed trend. It was confirmed that time duration has no relation with viability in case of graphene.

4.2.13 OD590 - Carbon Nanoclay - L929

In case of Nanoclay, the OD readings at 1:1 dilution are very low, almost zero, but with increase in dilution it increases markedly. The high cytotoxicity might be due to its fine powdery form. The increase in the OD reading is constant which gradually starts stabilizing at around 1:16 dilution. The effect of time duration does not show a fixed trend. If we see closely, its behaviour is similar to graphene. The reason for this can be attributed to the similarity in their forms. Both graphene and nano clay are very fine powders and dissolve the same way into the medium.

4.2.14 OD590 - Fullerene - L929

Fullerene shows a rather wider range of OD readings. There is a slight increase in the value of the OD readings with increase in dilutions but it is not very marked. More or less, it seems like the cytotoxicity of fullerene does not depend on the dilution. This feature is similar to the one seen in carbon nanowire. In case of fullerene, even though it is in a powder form, structure is a truncated icosahedron (covered in Chapter 2), made of twenty hexagons and twelve pentagons, with a carbon atom at the vertices of each polygon and a bond along each polygon edge. It is in the shape of a ball with very small bond length (1.4 angstroms) and hence does not have any open ends. It is similar in the way the nanotubes in carbon nanowire are threaded together and are not left free. OD readings, the readings for fullerene seem more haphazard. This might be due to the reason that fullerene is sparsely soluble in the medium due to which its cytotoxic effect on the medium is inconsistent. The cytotoxicity fullerene and its behaviour are in accordance to the studies by Jia et.al. (2005) [53]. In this study the cytotoxicity of carbon nanotubes are compared to that of fullerene by doing MTT tests on guinea pigs. According to her study fullerene induced injury at higher doses as compared to carbon nanotubes. After converting the OD readings to viability vs dilution graphs, they have been presented further.

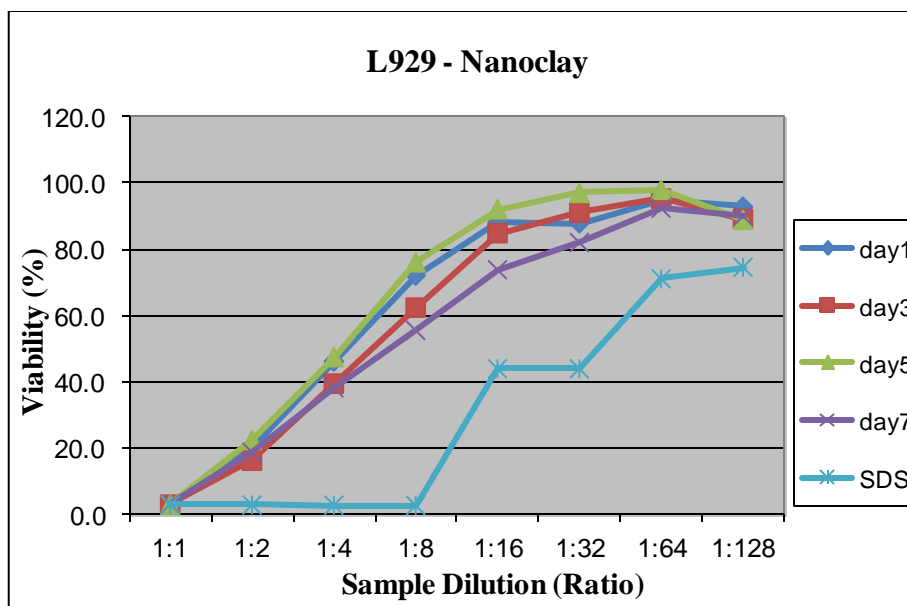


Figure 4.11: Graph showing the Viability vs Sample Dilution of Nanoclay on L929 cells.

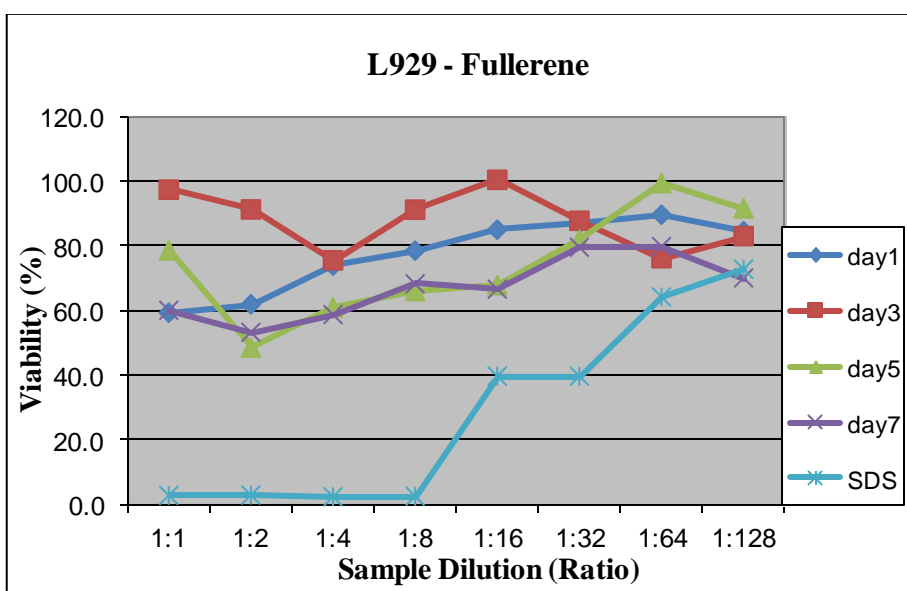


Figure 4.12: Graph showing the Viability vs Sample Dilution of fullerene on L929 cells.

4.2.15 Viability Graph- Nanoclay - L929

As shown in the graph above (Fig. 4.8), with increase in dilution, the viability of nanoclay increases. It is almost 0% at 1:1 dilution and increases to almost 90% at 1:32 and 1:64 dilution levels. This means that they can be used in the vicinity of live cells only over a dilution of 0.58mg/ml. The time duration does not show any fixed trend. There is no substantial difference between the curves of days 1, 3, 5 and 7. As mentioned earlier, its

behaviour is similar to graphene. Nanoclay like graphene has a high aspect ratio where the platelet thickness is around 1 nm and the surface dimensions are around 300-600 nm. Because of this it is capable of slicing through healthy live cells and kills them. Moreover, nanoclay is hydrophilic because of which they disperse readily in medium and easily interact with cells [62]. Hydrophilicity plays an important role in cell interaction. According to a paper by Ghosh the hydrophilicity can be adjusted to increase or decrease the interaction of nanomaterial with cells.

4.2.16 Viability Graph- Fullerene - L929

In case of fullerene (fig. 4.9), as seen above, the viability remains more or less the same with increase in dilution. The reason for this has been discussed in the section 4.2.13. There does not seem to be any relation between the time duration and the OD readings. Due to its very low solubility and negative charge is difficult to keep it dispersed in the medium for prolonged times to get a relation between OD reading and time duration. This behaviour was in sync with the behaviour described by Partha et.al [63] in his paper, where he discusses the hydrophobic nature and the cytotoxicity of fullerene based nanoparticles. In the paper their low level of cytotoxicity is attributed to their hydrophobic nature and chemical arrangement. Hence the graph points are more scattered. According to the average values calculated, the viability is over the safe range (>80%), beyond 1:8 dilution, i.e below 1.10mg/ml.

According to the studies conducted by Asmatulu [64] it has been confirmed the surface chemistry of particles at nanoscale, like surface charge and zeta potential play an important role due to the high surface area to volume ratio [64-71]. There are a number of factors which govern the chemical stability and behaviour of nanoparticles in a medium. The aggregation of nanoparticles is governed by the intermolecular interactions, like electrostatic, hydrophobic and Vander waals. Fullerene due to the hydrophobic behaviour and negative charge did not completely disperse in the medium. Carbon nanotubes also are known to have

some hydrophobic property due to which their level of cytotoxicity was lesser than graphene. It has also been reported by another study that shape and size of carbon based nanomaterials is an important factor in determining its cytotoxicity. Some carbon based nanomaterials with high aspect ratio, like carbon nanotubes, graphene, nanoclay etc.; have needle like fibre shapes and are structurally similar to asbestos as reported in the paper titled “Toxicity of Nanomaterials and Recent Developments in Protection Methods” by Asmatulu et.al. The higher the aspect ratio the higher is their ability to pierce through cells and increase the level of cytotoxicity. It has been reported in studies conducted by Karakoti et.al [66] and O’Brien et.al. [67] individually that smaller particles diffuse faster into the cells and cause cell damage as compared to larger particles. This effect as was seen in of graphene and nanoclay. It was more apparent in case of graphene because of the wide range particle distribution of the sample used. The recorded cytotoxicity of graphene was the highest on day 1 and the lowest on day 10, for both 3T3 and L929 cell cultures.

CHAPTER 5

CONCLUSION

This study compared the cytotoxicity levels of five different nanomaterials on 3T3 (mouse fibroblast) and L929 (human fibroblast) cancerous cells. The effects of cytotoxicity on both the cell types were similar in many ways but not identical. As compared to the mouse fibroblast cells, the human fibroblast cells have a larger surface area. Due to this reason, the viability values of L929 cells at different dilutions and time durations, varied over a wider range.

Out of the five Nanomaterials tested, pristine 100 ply carbon nanowire was the least cytotoxic nanomaterial with the average viability value being as high as 86.9%. This result was quite contrasting to the results reported in many of the previous cytotoxicity studies of nano materials. The effect of dilution on cytotoxicity of carbon nanowire was minimal. The reason for this effect was because of the single dimensional threaded structure of the nanowire, which is made by tightly twisting nanotubes together into a single unit. These nanotubes are not free to disperse into the medium (DMEM) and hence the total amount of medium in contact with the external surface of the nanowire remains the same. Contrastingly, it was noticed that with increase in time duration, the viability of this nanowire marginally went down. The reason for this behaviour might be because with increased soaking time the threaded structure unwinds itself and becomes weaker. The nanotubes from this structure separate and disperse into the medium and raise the level of cytotoxicity. The concentration of carbon nanowire at which it showed this high value of viability (86.9%) was $3\text{cm}^2/\text{ml}$ (external surface area cm^2/ml) which weighed 18.52 mg/ml.

The second most viable material after carbon nanowire was fullerene with a viability value of 75.2%. The close packed truncated icosahedron structure, with no open bonds is one of the main reasons for its stability in medium. It is also known to show a negative

charge and is hydrophobic, which decreases its soluble in the medium in an aggregated state. The maximum concentration at which fullerene showed viability was 10.00 mg/ml for a viability over 70% and 2.00 mg/ml for a viability over 80%. The viability of other nano materials were in the order carbon nanotubes (69.75%), graphene (67.48%) and nanoclay (61.34%). These nanomaterials, because of their fine powdery nature and higher hydrophilicity, are easily dispersed into the medium. They have a very high aspect ratio which makes it easy for these needle-like structures to cut through the cells and kill them. It was observed that with decrease in the concentration there was a steep increase in the viability. The maximum concentration for these nanomaterials was calculated to be 1.01 mg/ml for over 70% viability and 0.58 mg/ml for over 80% viability.

CHAPTER 6

FUTURE WORK

A lot of future work can be developed from the existing study. Since the viability of carbon nanowire reduces on prolonged contact with medium, the wire can be functionalized and tested for its stability in a medium. Cytotoxicity tests can also be conducted on other types of cells, such as, human lung cells and red-blood cells. Furthermore, in-vivo tests can be performed on mice to get more insight into its biocompatibility. On the other side, the cytotoxic materials like carbon nanotubes, nanoclay and graphene can be tested on disease causing bacteria or viruses to see their cytotoxic effects on them. They may be useful materials to treat many diseases, as well.

REFERENCES

LIST OF REFERENCES

- [1] Park H.S., Cai W., Espinosa H.D., Huang H., “Mechanics of Crystalline Nanowires”, *MRS Bulletin*, 2009, Vol. 34, Issue 3, pp 178-183.
- [2] Kiuchi M., Isono Y., Sugiyama S., Morita T., “ Mechanical and electrical properties evaluation of carbon nanowire using electrostatic actuated nano tensile testing devices (EANAT)”, *5th IEEE Conference on Nanotechnology Japan*, 2005, Vol. 2, pp 486 – 489.
- [3] Jia G., Wang H. , Yan L., Wang X., Rong P. J., Yan T., Zhao Y., Biaoguo X., “Cytotoxicity of Carbon Nanomaterials: Single-Wall Nanotube, Multi-Wall Nanotube, and Fullerene”, *Environmental Science and Technology Journal*, 2005, Vol. 39, Issue 5, pp 1378–1383.
- [4] Wang K., Ruan J., Song H., Zhang J., Wo Y., Guo S., Cui D., “Biocompatibility of Graphene Oxide”, *Nanoscale Research Letters*, 2011, Vol. 6, pp-8.
- [5] Bakry R., Vallant R.M., Najam-ul-Haq M., Rainer M., Szabo Z., Huck C.W., Bonn G.K., “Medicinal Applications of Fullerenes”, *International Journal of Nanomedicine*, 2007, Vol. 2, Issue 4, pp 639–649.
- [6] Morgan A. B. “Nanoclays for Composites”, *Material Matters*, 2007, Vol. 2, pp 20.
- [7] Giannelis E. P., “Nanoclays for Composites” *Advanced Materials*, 1996, Vol. 8, pp 29.
- [8] Vaia R. A, Jandt K.D., Kramer E., Giannelis E. P.,” Nanoclays for composites” *Chem. Mater.*, 1996, Vol 8, pp 2628.
- [9] LeBaron, P. C., Wang, Z., Pinnavaia, T. J., “Nanoclays for composites “, *Applied Clay Science*, 1999, Vol. 15, pp 11.
- [10] Dresselhaus M.S., Dresselhaus G., Avouris P., “*Carbon Nanotubes: Synthesis, Structure, Properties, and Applications*”, Springer, April 2001, pp 12.
- [11] Baughman R.H., Zakhidov A.A., Heer W.A.,” Carbon Nanotubes- The route towards Applications”, *Science*, 2002, Vol. 297, Issue 5582, pp. 787-792.
- [12] O'Connell M.J., “*Carbon nanotubes: properties and applications*”, CRC Press, May 2006, pp 21.
- [13] Park S., An J., Jung I., An S.J., Li X., Velamakanni A., and Ruoff R.S., “Colloidal Suspensions of Highly Reduced Graphene Oxide in a Wide Variety of Organic Solvents”, *Nano Lett.*, 2009, Vol. 9, Issue 4, pp 1593–1597.

- [14] Hsuan K., Liao, Lin Y.S., Macosko C.W. and Haynes C.L., “Cytotoxicity of Graphene Oxide and Graphene in Human Erythrocytes and Skin Fibroblasts”, *ACS Appl. Mater. Interfaces*, 2011, Vol. 3, Issue 7, pp 2607–2615.
- [15] Akhavan O. and Ghaderi E., “Toxicity of Graphene and Graphene Oxide Nanowalls against Bacteria”, *ACS Nano*, 2010, Vol. 4, Issue 10, pp 5731–5736.
- [16] Prato M., “Fullerene Chemistry for Materials Science Applications”, *J. Mater. Chem.*, 1997, Vol. 7, 1097-1109.
- [17] Hirsch A., “*The Chemistry of Fullerenes*”, WILEY-VCH Verlag GmbH, 2008, pp 2-7.
- [18] Lau K., Gu C., Hui D. “A Critical Review on Nanotube and Nanotube/Nanoclay related polymer composite materials”, *Nanoengineered Composites and Ceramic Laminates*, 2006, Vol. 37, Issue 6, 2006, pp 425–436.
- [19] Promega- <http://www.promega.com/resources/product-guides-and-selectors/protocols-and-applications-guide/apoptosis/>- Taken on March 13th 2012.
- [20] Riss T.L. and Moravec R.A., "Use of multiple assay endpoints to investigate the effects of incubation time, dose of toxin, and plating density in cell-based cytotoxicity assays", *Assay Drug Dev Technol*, February 2004, Vol. 2, Issue 1, pp 51–62.
- [21] XENOMERIX, BioAntares LLC, San Francisco CA, http://www.bioantares.com/Cytotoxicity_Screening.html – taken on March 27th 2012
- [22] Freshney R. “Culture of Animal Cells: A Manual of Basic Technique”, *Alan R. Liss Inc.*, New York, 1987, pp 117
- [23] Judith R. “The Evaluation of Trypan Blue Technique for Determination of Cell Viability”, *The Journal of Transplantation Society*, 1964, Vol. 2, Issue 6
- [24] Bio- science Laboratory Inc, <http://www.biosciencelabs.com/pages/27/Virology.html> – taken on March 27th 2012
- [25] Sigma-Aldrich, Material Safety Data Sheet, Version 4.2, Revision Date 01/19/2012, Print Date 03/28/2012- – taken on March 27th 2012
- [26] Lobner D. “Comparison of the LDH and MTT assay for quantifying cell death: validity for neuronal apoptosis”, *Journal of Neuroscience Methods*, 2000, Vol. 96, Issue 2, pp 147-152.
- [27] Lab tests Online- <http://labtestsonline.org/understanding/analytes/ldh/tab/test> – taken on March 20th 2012
- [28] Vichai V. and Kirtikara K., “Sulforhodamine B colorimetric assay for cytotoxicity screening”, *Nature Protocols*, 2006, Vol. 1, 1112 - 1116

- [29] Houghton P., Fang R., Techatanawat I., Steventon G., Hylands P.J., Lee C., “The sulphorhodamine (SRB) assay and other approaches to testing plant extracts and derived compounds for activities related to reputed anticancer activity.”, Elsevier, 2007, Vol 42, Issue 4, pp 377-87
- [30] Voigt W., “Sulforhodamine B assay and Chemosensitivity.” *Biomedical and Lifescience SpringerLink*, 2005, Vol. 110, pp 39-48.
- [31] EMD Millipore - <http://www.millipore.com/cellbiology/cb3/wst-1> - taken on February 28th 2012
- [32] Biosciences- <http://www.gbiosciences.com/CytoScanWST1-desc.aspx> - taken on February 28th 2012
- [33] Nicolaas, Franken A.P., Rodermond H.M., Stap J., Haveman J. and Bree C.V., “Clonogenic assay of cells in vitro”, *Nature Protocols*, December 2006, Vol 1, pp 2315 – 2319
- [34] Hoffman R.M., “In vitro sensitivity assays in cancer: A review, analysis, and prognosis”, *Journal of Clinical Laboratory Analysis*, 1991, Vol. 5, pp 133-143
- [35] Keese C.R., Wegener J., Walker S.R. and Giaever I., “Electrical wound-healing assay for cells in vitro”, *PNAS*, February 2004, Vol. 101, Issue 6, pp 1554-1559
- [36] ATCC- Life Science Research
<http://www.atcc.org/CulturesandProducts/CellBiology/KitsPanels/MTTCellProliferationAssay/tabid/569/Default.aspx> - Taken on March 20th 2012
- [37] Ahmadian S., Barar J., Saei A.J., Fakhree M.A.A. and Omid Y., “Cellular Toxicity of Nanogenomedicine in MCF-7 Cell Line: MTT assay”, *Journal of Visualized Experiments*, 2009- Video
- [38] Swing R.E., “*An Introduction to Microdensitometry*”, SPIE Society for Optical Engineering, 1998, pp 3-4
- [39] Optical density, Spectroscopy science – Britannica online encyclopedia. Taken on March 27th 2012
- [40] Muller J., Huaxa F., Moreaub N., Missona P., Heiliera J.F. and Delosc M., “Respiratory toxicity of multi-wall carbon nanotubes.”, *Toxicology and Applied Pharmacology*, 2005, Vol 207, pp 221-231
- [41] Smart S.K., Cassady A.I., Lu G.Q. and Martin D.J., “The biocompatibility of carbon nanotubes.”, *Toxicology of Carbon Nanomaterials*, May 2006, Vol 44, Issue 6, pp 1034–1047

- [42] Stoker E., Purser F., and Kwon S., “Carbon Nanotubes Using Three-Dimensional Tissue-Engineered Human Lung”, *International Journal of Toxicology*, Nov 2008, Vol 27, Issue 6, pp 441-448
- [43] Davoren M., Herzog E., Casey A., Cottineau B., Chambers G., Byrne H.J. and Lyng F.M., “In vitro toxicity evaluation of single walled carbon nanotubes on human A549 lung cells”, *Toxicology in Vitro*, April 2007, Vol 21, Issue 3, pp 438–448
- [44] Wang K., Ruan J., Song H., Zhang J., Wo Y., Guo S. and Cui D., “Bio Compatibility of Graphene oxides”, *Nanoscale Research Letters*, 2011, Vol 6, Issue 8.
- [45] Sanhes L., Tang R., Delmer A., DeCaprio J.A. and Ajchenbaum-Cymbalista F., “Fludarabine-Induced Apoptosis of B Chronic Lymphocytic Leukemia Cells Includes Early Cleavage Of P27kip1 By Caspases” *Leukemia*, 2003, Vol. 17, pp 1104–1111
- [46] Tian F. , Cui D., Schwarz H., Estrada G.G. and Kobayashi H., ‘Cytotoxicity of single-wall carbon nanotubes on human fibroblasts’, *Toxicol In Vitro*, 2006, Vol. 20, Issue 7, pp 1202-1212
- [47] Zhang Y., Ali S.F., Dervishi E., Xu Y., Li Z., Casciano D. and Biris A.S., “Cytotoxicity Effects of Graphene and Single-Wall Carbon Nanotubes in Neural Phaeochromocytoma-Derived PC12 Cells”, *ACS Nano*, June 2010, Vol 4, Issue 6, pp 3181-3186
- [48] Bottini M., Bruckner S., Nika K., Bottini N., Bellucci S., Magrini A., Bergamaschi A., Mustelin T., “Multi-walled carbon nanotubes induce T- lymphocyte apoptosis”, *Toxicology Letters*, 2006, Vol 160, pp 121-126
- [49] Kalbacova M., Kalbac M., Dunsch L., Kataura H., and Hempel U., “The study of the interaction of human mesenchymal stem cells and monocytes /macrophages with single-walled carbon nanotube films”, *Physica Status Solidi*, 2006, Vol 243, Issue 13, pp 3514-3518
- [50] Muller J., Decordier I., Hoet P.H., Lombaert N.M., Thomassen L., Huaux F., Lison D. and Volders M.K. “Clastogenic and aneugenic effects of multi-wall carbon nanotubes in epithelial cells”, *Carcinogenesis*, 2008, Vol 29, Issue 2, pp 427-433.
- [51] Cherukuri P., Bachilo S.M., Litovsky S.H. and Weisman R.B., “Near-Infrared Fluorescence Microscopy of Single-Walled Carbon Nanotubes in Phagocytic Cells”, *Carcinogenesis*, 2008, Vol 29, Issue 2, pp 427-433
- [52] Shvedova A., Castranova V., Kisin E., Schwegler-Berry D., Murray A., Gandelsman V., Maynard A., and Baron P., ”Exposure to Carbon Nanotube Material: Assessment of Nanotube Cytotoxicity using Human Keratinocyte Cells”, *Journal Toxicol Environ Health A.*, October 2003, Vol 66, Issue 20, pp 1909-1926
- [53] Jia G., Wang H., Yan L., Wang X., Pei R., Yan T., Zhao Y. and Guo X., “Cytotoxicity of Carbon Nanomaterials: Single-Wall Nanotube, Multi-Wall

- Nanotube, and Fullerene”, *Environ. Sci. Technology*, 2005, Vol 39, Issue 5, pp 1378–1383
- [54] Sharifi S., Behzadi S., Laurent S., Forrest M.L., Stroeve P. and Mahmoudi M. “Toxicity of Nanomaterials”, *Chem. Soc. Rev.*, 2012, Vol 41, pp 2323-2343
- [55] Deng Z.J., Liang M.T., Monteiro M., Toth I. And Minchin R.F., “Nanoparticle-induced unfolding of fibrinogen promotes Mac-1 (CD11b/CD18) receptor activation and pro-inflammatory cytokine release”, *Nature Nanotechnology*, 2011, Vol. 6, pp 39–44
- [56] Sato Y., “Influence of length on cytotoxicity of multi-walled carbon nanotubes against human acute monocytic leukemia cell line THP-1 *in vitro* and subcutaneous tissue of rats *in vivo*”, *Molecular Biosystems*, July 2005, Vol 1, Issue 2, pp 176-182
- [57] Akhavan O. and Ghaderi E., “Toxicity of Graphene and Graphene Oxide Nanowalls Against Bacteria”, *ACS Nano*, 2010, Vol 4, Issue 10, pp 5731–5736
- [58] United States Environment Protection Agency, EPA 620/K-09/011, June 2009, www.epa.gov/nanoscience.
- [59] Pulskamp K., Diabaté S., Krug H.F., “Carbon nanotubes show no sign of acute toxicity but induce intracellular reactive oxygen species in dependence on contaminants”, *Toxicology Letters*, January 2007, Vol 168, Issue 1, pp 58-74
- [60] Nanocor, AMCOL International Corporation, http://www.nanocor.com/nano_struct.asp taken on 15th April 2012
- [61] Robert R., Mc Cormick School of Engineering and Applied Science, Department of Mechanical Engineering, Advanced Materials Lab, Synthesis and Characterization of Nanoreinforced Polymers. <http://www.mech.northwestern.edu/fac/brinson/new/research/nanosynthesis.php> taken on 15th April 2012
- [62] Ghosh P.K., “Hydrophilic polymeric nanoparticles as drug carriers”, *Indian Journal of Biochemistry and Biophysics*, Oct 2000, Vol 37, pp 273
- [63] Partha R., Mitchell L.R., Lyon J.L., Joshi P.P., Conyers J.L., “Buckysomes: fullerene-based nanocarriers for hydrophobic molecule delivery.” *ACS Nano*, 2008, Vol. 2, Issue 9, pp 1950-1958.
- [64] Asmatulu, R. “Toxicity of Nanomaterials and Recent Developments in Lung Disease,” Chapter 6 in *Bronchitis*, InTec, ed. P. Zobic, 2011, pp. 95-108.
- [65] Asmatulu, R., Asmatulu, E. and Yourdkhani A. “Toxicity of Nanomaterials and Recent Developments in Protection Methods”, *Proceedings Midwest Section Conference of the American Society for Engineering Education*, Lawrence KS, 2010, pp 22-24

- [66] Karakoti A.S., Hench L.L., and Seal S., "The Potential Toxicity of Nanomaterials-The Role of Surfaces", *Journal of the Minerals*, 2006, pp 77-82.
- [67] O'Brien N. and Cummins E., "*Nanomaterials: Risks and Benefits*", Springer Netherlands, 2008, pp 161-178.
- [68] Asmatulu R., and Misak H. "Hands-On Nanotechnology Experience in the Collage of Engineering at Wichita State University: A Curriculum Development," *Journal of Nano Education*, Vol. 3, 2012, pp. 1-11.
- [69] Asmatulu, R., Asmatulu, E., and Zhang, B. "Recent Progress in Nanoethics and Its Possible Effects on Engineering Education," (in press, *International Journal of Mechanical Engineering Education*).
- [70] Asmatulu, R., Garikapati, A., Misak, H.E., Song, Z., Yang, S.Y., and Wooley, P.H. "Cytotoxicity of Magnetic Nanocomposite Spheres for Possible Drug Delivery Systems," *ASME International Mechanical Engineering Congress and Exposition*, Vancouver, Canada, November 12–18, 2010, 8 pages.
- [71] Asmatulu, R., Asmatulu, E., and Yourdkhani, A. "Toxicity of Nanomaterials and Recent Developments in the Protection Methods," *SAMPE Fall Technical Conference*, Wichita, KS, October 19–22, 2009, 12 pages